EUROPEAN FUSION DEVELOPMENT AGREEMENT

EFDA–JET–PR(04)52

G. Saibene, R. Sartori, A. Loarte, P.J. Lomas, V. Parail, K.D. Zastrow, Y. Andrew, S. Sharapov, A. Korotkov, D.C. McDonald, K. Guenther, A.G. Meigs, S.A. Arshad, M. Becoulet, P.R. Thomas, P. Monier-Garbet, F.G. Rimini, H.R. Koslowski, C.P. Perez, J. Stober, G.D. Conway, M.A.H. Kempenaars, L.C. Ingesson, J.S. Lönnroth[7] and JET EFDA contributors

Characterisation of Small ELM Experiments in Highly Shaped Single Null and Quasi-Double Null Plasmas in JET

Characterisation of Small ELM Experiments in Highly Shaped Single Null and Quasi-Double Null Plasmas in JET

G. Saibene[1], R. Sartori[1], A. Loarte[1], P.J. Lomas[2], V. Parail[2], K.D. Zastrow[2], Y. Andrew[2], S. Sharapov[2], A. Korotkov[2], D.C. McDonald[2], K. Guenther[2], A.G. Meigs[2], S.A. Arshad[2×], M. Becoulet[3], P.R. Thomas[3], P. Monier-Garbet[3], F.G. Rimini[3], H.R. Koslowski[4], C.P. Perez[4], J. Stober[5], G.D. Conway[5], M.A.H. Kempenaars[6], L.C. Ingesson[6+], J.S. Lönnroth[7] and JET EFDA contributors*

[1]EFDA Close Support Unit, Boltzmannstr. 2, 85748 Garching, Germany
[2]Association Euratom/UKAEA, Culham Science Centre, Abingdon OX14 3EA, UK
[3]Association Euratom/CEA, Cadarache, F13108 St. Paul-lez-Durance, France
[4]Forschungszentrum Jülich GmbH, Institut für Plasmaphysik, EURATOM Association, Trilateral Euregio Cluster, 52425 Jülich, Germany
[5]Association Euratom/IPP, MPI fur Plasmaphysik, 2 Boltzmannstrasse, Garching, Germany
[6]FOM/Euraton instituut v plasmaphysica 'Rijnhuizen', Nieuwegein, Trilateral Euregio Cluster, The Netherlands
[7]Association EURATOM-tekes, Helsinki Univ of Technology, PO Box 2200, 02015 HUT, Finland
[×]also EFDA Close Support Unit JET, Culham Science Centre, Abingdon OX14 3EA, UK
[+]also EFDA Close Support Unit, Boltzmannstr. 2, 85748 Garching, Germany
** See annex of J. Pamela et al, "Overview of Recent JET Results and Future Perspectives", Fusion Energy 2002 (Proc.19 th IAEA Fusion Energy Conference, Lyon (2002).*

Preprint of Paper to be submitted for publication in
Nuclear Fusion

ABSTRACT

This paper describes experiments with highly shaped JET H-mode plasmas, that where directed to developing regimes where Type I ELMs are replaced by other edge relaxations, while maintaining the pedestal pressure of Type I ELMy H-modes. It was found that Type II ELMs coexisted with Type I, up to densities of the order of the Greenwald limit, where Type III ELMs appear, and the good confinement was lost. Only at the highest edge collisionality was it observed that Type II ELMs completely replace Type I. At high β_p and q_{95}, "grassy" ELMs replace Type I completely. The MHD spectra chacteristics for grassy ELMs are significantly different from those of Type II ELMs. The paper details the experiments, briefly compared the results to those obtained elsewhere, and suggests open lines of investigations for the assessment of the potential of grassy ELM regimes as ELM mitigation technique.

1. INTRODUCTION

Access conditions and plasma performance of H-modes with acceptable ELM size (extrapolated to ITER conditions, [5]) have been one of the main research lines in recent experimental campaigns at JET . This paper describes experiments dedicated to the study of pedestal and ELM behaviour of high density/high confinement ELMy H-modes [19], [11], focussing on the exploration of access conditions for small ELM regimes without the use of "external actuators", such as repetitive pellet injection [10] or edge magnetic perturbation coils [4], etc.

Regimes combining high global confinement, high pedestal pressure p_{ped} and small ELMs have been achieved in ASDEX-Upgrade and JT-60U: in both cases, a spontaneous transition from a standard ELMy H-mode edge is observed, in response to changes in some specific plasma parameters. In the case of ASDEX-Upgrade, [24] Type II ELMs replace Type I ELMs when the plasma magnetic configuration is changed from lower Single Null (SN) to Quasi Double-Null (QDN). High pedestal density ($n_{ped} > 6$ " $710^{19}m^{-3}$ or 60 - 70%n_{GR} with $n_{GR} = I_p/\pi a^2$, $10^{20}m^{-3}$MA, I_p = plasma current and a = plasma minor radius [Greenwald et al., 1988]), edge safety factor $q_{95} > 4.0$ - 4.5 at $\beta_N \sim 1.8$ - 2.2 and high triangularity are also required for the transition to take place, but they are not sufficient conditions. In the case of JT-60U [Kamada et al., 2002], high triangularity ($\delta \sim 0.45$ to 0.7) ELMy H-modes with medium-high q_{95} ($q_{95} \sim 3.8$ to 6) enter a regime characterised by high p_{ped} and small ELMs (named "grassy ELMs" regime) when a β_p threshold of ~ 1.6 - 1.7 is exceeded. In both regimes, the suppression of type I ELMs does not lead to significant changes of the global particle confinement or impurity transport, indicating that additional transport mechanisms replace the bursty losses of Type I ELMs.

Simultaneous high confinement and density are routinely achieved in steady state conditions for ~ $20\tau_E$ in JET with highly shaped plasmas. The normalised parameters required for the Q = 10 inductive operation of IT ER, namely $H_{98} \sim 1$, density > 85%n_{GR} and $\beta_N \sim 2$ with $q_{95} \sim 3$ - 3.6, are obtained in lower SN plasmas, with average triangularity at the separatrix $\delta \sim 0.4$ - 0.5. These plasmas are characterised by an external transport barrier and Type I ELMs. As described in [19],

increasing the pedestal density n_{ped} above a critical value (typically n_{ped} > 70% - 80% n_{GR}) at constant plasma parameters, results in a reduction of the Type I ELM frequency f_{ELM} down to a few Hz, while Type I ELM prompt energy losses do not increase or even decrease compared to those of Type I ELMs of the same frequency but at lower density. This change in the Type I ELM behaviour occurs at constant (or slightly increased) plasma confinement (H_{98} is not any longer decreasing with density [18]) and pedestal pressure, up to $n_{ped} \sim n_{GR}$. Global power balance shows that the reduction in f_{ELM} is accompanied by enhanced energy and particle losses between ELMs, attributed to the presence of an additional edge loss mechanism, identified, by analogy with other experiments, as Type II ELMs. Type II ELMs in JET are characterised by specific and reproducible changes in the spectrum of MHD fluctuations, namely by an increase of broadband fluctuations in the 10-40kHz range [19] compared to similar plasmas having pure Type I ELMs. These broadband fluctuatons are identified as strong Wash Board modes [13]. In the Type II ELM phases, the temperature T_{ped} at the top of the pedestal reaches saturation, while the raise rate of n_{ped} is reduced, but does not go to zero, eventually leading to a stability limit and a Type I ELM. As reported in [19], initial experiments to improve the mixed Type I-II regime up to total Type I ELM suppression were not successful in JET; in particular attempts at increasing even further the plasma edge density lead to a transition to Type III ELMs and reduced plasma confinement.

1.1 THE EXPERIMENTS

As outlined in section 1, this paper presents the results of a series of experiments investigating the behaviour of the plasma pedestal and ELMs in high density/high confinement ELMy H-modes in JET, and the access to small ELM regimes. The full set of H-mode diagnostics available in JET was exploited in these experiments, including fast ECE, magnetics and reflectometry measurements. Profile data were acquired with core and edge charge-exchange diagnostics for T_i measurements, edge and core LIDAR for n_e and T_e data. For a detailed description of the characteristics of the diagnostic used for H-mode physics studies in JET, please refer to [19].

The investigation focussed on three main set of experiments using several different plasma configurations that are briefly described in Table 1, together with some general parameters covered in the study. The following experiments were carried out: (see Table 1.)

1. The exploration of the effects of the plasma boundary magnetic geometry (triangularity δ, as well as proximity to Double Null) and of q_{95} on global confinement, pedestal parameters, ELM type and losses. These experiments were aimed at obtaining a steady-state Type II ELM regime for typical JET H-mode plasma parameters, and at the study of access conditions by direct comparison of pedestal and ELM characteristics in high δ SN and QDN plasmas, in similar experimental conditions. The experiments were carried out mainly in two configurations: a SN configuration named HT3 and a high δ, high elongation, Quasi Double Null configuration called QDN1 (see Table 1). Additional heating was a combination of dominant NB injection (13 - 16MW), with the addition of 2 - 3MW of central ICRH (H

minority heating). In QDN , machine safety considerations (in particular issues of plasma vertical stability to large type I ELMs in highly elongated plasmas) restricted operations to high density, where the Type I ELM size is reduced, and fast vertical excursions of the plasma more easily controlled. The results of these experiments are presented in section 2.

2. The investigation of the role of proximity to Double Null for achieving Type II ELM H-modes, in an dimensionless identity experiment with ASDEX-Upgrade, [24]. For this experiment, the QDN1 configuration was adapted to match the average δ and κ and Δ_{sep} of a Type II ELM discharges in ASDEX-Upgrade and the plasma current and field were scaled to obtain a dimensionless identity with our model ASDEX-Upgrade Type II H-mode plasma. This identity, for JET, is a plasma at 0.87MA/1.17T, with average $\delta \sim 0.44$ and a QDN configuration (QDN-sim, Table 1) with $\Delta_{sep} \sim 1$cm, and this was kept fixed for this experiments. As in ASDEX-Upgrade, neutral beams were the dominant additional heating (up to ~ 4MW), with small amounts of ICRH (H minority heating, central resonance, $\lesssim$ 1MW). In this geometry, the plasma current and magnetic field were increased at constant q_{95} to investigate the effect of varying pedestal parameters and H-mode threshold on Type II ELM access.

3. The study of the effect of β_p on the pedestal and ELM activity, in analogy with JT-60U, where "grassy ELMs" spontaneously replace Type I ELMs in H-modes, when a threshold value of β_p is exceeded ($\beta_p > 1.7$). In JT-60U, high q_{95} and δ are also required to access the Grassy ELM regime, but a trade-off has been identified experimentally between the value of the safely factor and shape, [7]. In contrast to the JET/ASDEX-Upgrade identity, no attempt was made in these experiments to obtain a dimensionless match in JET of the JT-60U plasma parameters, with the exception of β_p. In particular, the experiments in JET were carried out in plasmas with a fully penetrated current profile, no ITB and QDN magnetic geometry. β_p was increased in steps from 1.1 to 1.9, by increasing the input power (combined NB and H minority central ICRH) and, at the maximum input power, reducing the plasma current at fixed field. The results from these experiments are described in section 3 and compared to standard ELMy H-modes at low β_p ($\beta_p < 1$) and to a series of discharges at low l_i but the same current and field, 1.2MA/2.7T, and with β_p in the same range ~1.1 to ~1.9 as the high-l_i H-modes. The low-l_i H-modes used current profile control to obtain plasmas with $q_0 > 2$ and broad current profile ($l_i \sim 0.85$). The discharges are standard lower SN, with the same δ, κ and similar q_{95} as the QDN high β_p described above.

2. COMPARISON OF HIGH δ SINGLE AND QUASI-DOUBLE NULL H-MODES FOR VARIABLE q_{95}

This section compares the results of the studies of H-mode characteristics and ELM behaviour of highly shaped plasmas SN and QDN plasmas in JET. In particular, paragraph 2.1 analyses the global confinement, pedestal and ELM characteristics of the HT3 and QDN1 configurations. Most

of the experiments were carried out at 2.5MA/2.7T, with β_N ~ 1.8 - 2.0. As shown in Table 1, this combination of current and field correspond to edge safety factors between 3 and 3.6, depending on the plasma minor radius of the different configurations; a series of experiments was also carried out to study the effect of the edge safety factor on Type II ELM access both in SN and QDN, varying q_{95} from 3.6 $\rightarrow$ 4.6 and 3.0 $\rightarrow$ 4.1 respectively. In contrast to earlier experiments (see, for instance, [19]), the variation of the safety factor in SN was achieved by varying the toroidal field at constant plasma current. This choice was motivated by the observation of the ~ I^2_p dependence of the pedestal pressure of JET ELMy H-modes (not strongly dependent on q_{95}, for the range of q_{95} investigated in this paper, [11]). In these conditions it was thought that any change in the ELM behaviour with q would be easier to interpret. The observations related to the onset of Type II ELMs for these experiments are summarised in paragraphs 2.2 and 2.3, while the results of the JET/ASDEX-Upgrade dimensionless identity with a QDN plasma shape are described in paragraph 2.4.

2.1 CONFINEMENT AND PEDESTAL PARAMETERS

The role of the second null in determining the onset of Type II ELMs was investigated by varying the first-to-second separatrix distance Δ_{sep}, moving the plasma vertically upwards in 4 fine steps in 4 separate pulses. The equilibria corresponding to each pulse/Δ_{sep} value are shown in Fig. 1, while the poloidal distribution of radiation for each case is shown in Fig. 2. While the stronger radiation emission is in the lower x-point region for Δ_{sep} = 2cm, radiation from the upper x-point region increases as the plasma is moved upwards and Δ_{sep} reduced. For Δ_{sep} < 1cm, the upper x-point region dominates the radiation emission. On the other hand, power balance calculations carried out using the divertor thermocouples system indicate that the power flow is still predominantly conducted to the lower x-point region, even for the minimum Δ_{sep} (~ 35% maximum power deficit to the lower divertor). This indicates that, although the recycling pattern changes when reducing Δ_{sep}, the active divertor is still the lower one, even for the minimum Δ_{sep}.

It is found that, at 2.5MA and q_{95} ~ 3.0 to 3.6, the plasma enters the mixed Type I-II regime, for both SN and QDN configurations for $n_{ped} > 70\% - 80\% n_{GR}$, with typical Type I ELM frequency f_{ELM} of 6 to 10Hz, compared to ~ 15 - 20Hz of the unfuelled, lower n_{ped} cases. The lower f_{ELM} is measured for QDN plasmas, for otherwise similar plasma conditions. The overall similarity of the pedestal and ELM behaviour for SN and QDN plasmas in JET is illustrated in Fig. 3, by comparing selected time traces of No: 57987 (SN HT3) and of No: 59237 (QDN QDN1), both at 2.5MA/2.7T. Pulse No: 59237 has Δ_{sep} ~ 2cm, and it was selected because it produced the best performance, in terms of both core and pedestal parameters, of the series of QDN1 where Δ_{sep} was varied. The two pulses have almost identical input power and very similar gas fuelling: both reach extreme high densities with a mixed Type I-II H-mode edge. Figure 3 also exemplifies some of the differences between SN and QDN H-mode behaviour: for the same external fuelling, the QDN plasma reaches higher absolute densities in average and in the pedestal, although n/n_{GR} is similar for the two pulses. In general, approaching a double-null configuration reduces, by up to a factor of ~ 2, the

amount of external fuelling required to reach a certain steady state n_{ped} compared to the HT3 plasmas, consistent with increased particle recycling from the upper x-point region and, possibly, deeper neutral penetration. The reduction of Δ_{sep} from ~ 2cm to quasi pure double null geometry, while the plasma pedestal is in the mixed Type I-II regime, does not result in the suppression of Type I ELMs, but rather in a reduction of p_{ped} and transitions to Type III ELMs. Although repetitive plasma pulses were successfully used to condition the upper x-point target, the lack of active pumping in the upper divertor region may affect the plasma response to external fuelling and possibly the observed ELM behaviour.

The confinement enhancement factor H_{98} for SN HT3 at 2.5MA/2.7T and that of QDN1 at same I_p/B_T are compared in Fig.4. Each point represents a plasma pulse and the shaded areas indicate pulses in the mixed Type I-II regime. The normalised confinement of the QDN plasmas is 10 to 20% lower than the reference HT3, for the same I_p and normalised n_{ped}. The lowest H_{98} values in QDN1 shape correspond to plasmas with the lowest Δ_{sep}, i.e. closest to pure double null. For both configurations, the core density profiles are weakly peaked (n_{core}/n_{ped} ~ 1.2), while QDN1 plasmas systematically reach higher absolute densities. The reduction of the normalised confinement mentioned above is not entirely accounted for by the predicted positive density dependence of H_{98} ($H_{98} \propto n^{+0.4}$ in the scaling) not found in the data, but also reflects the somewhat reduced plasma energy content compared to equivalent SN plasmas.

Experimental evidence from other devices shows that high edge safety factor ($q_{95} > 4$) facilitates the access to steady state Type II/Grassy ELM regimes (ASDEX-Upgrade, [24] and JT-60U, [8]). This was tested in the JET experiments, where q_{95} was increased in both SN and QDN configurations, and a gas scan and proximity to double null scan carried out. In the case of the SN , q_{95} was increased to 4.6 at constant I_p (experiments where q_{95} was increased at constant B_T for SN are reported in [19]), while for QDN1, due to limitations on the allowable power load to the upper x-point region, q_{95} was raised from 3.1 to 3.6 and then to 4.1 by decreasing I_p (i.e. without increasing the L - H power threshold, and therefore the required input power). As an example, time traces of two SN HT3 plasmas are compared in Fig.6: for the same plasma current, external fuelling and with equivalent input power (normalised to the the L $\rightarrow$ H transition power), the plasma with higher q_{95} (pulse No: 58111) has reduced confinement enhancement factor, reaches a lower density and has much more frequent Type I ELMs (f_{ELM} (58111) ~50 - 70Hz while f_{ELM} (57885) ~ 25Hz).

Figure 6 is an illustration of a general result: increasing q_{95}, for both SN and QDN results in a strong increase of the ELM frequency (by factor of 2 to 3) and, as also shown in Fig. 4, reduces the normalised confinement [20]. These results are similar and consistent with those reported in [19], where a q scan was carried out in SN by decreasing I_p at constant B_T. Moreover, the maximum pedestal (and core) density achievable before the type I-III ELM transition is substantially reduced compared to the lower q_{95} cases, from 90% down to 60 - 70%n_{GR}. On the other hand, the “optimal” q value for the access to the mixed Type I-II regime (i.e. to high density and high confinement)

depends on the plasma configuration: as Fig.4 shows, the best n - H_{98} combination is achieved in HT3 SN for q_{95} = 3.6 [21] while, increasing q_{95} above 3, already results in reduced performance in QDN configuration.

The behaviour of the pedestal parameters is consistent with the picture given by the confinement. The high confinement at high density obtained in the SN HT3 at q_{95} = 3.6 corresponds to a clamping of T_{ped} for increasing density, i.e. to an effective increase of the pedestal pressure with density and to the onset of mixed Type I-II ELMs. This is the case also for the QDN1 at low q_{95}, although T_{ped} is somewhat reduced compared to the SN plasmas, as is H_{98}, but it is not observed at higher q_{95}. Increasing q in SN results in a reduced pedestal pressure as well as in a transition to Type III ELMs at lower n_{ped} (Fig.5), compared to SN plasmas at the same I_p but with q_{95} ~ 3 - 3.6. As mentioned in section 1, the onset of mixed Type I-II ELMs is characterised by an anomaly in the frequency of Type I ELMs that, instead of increasing for increasing n_{ped} (at constant power across the separatrix), starts to decrease. In low q H-modes, this change of f_{ELM} occurs at n_{ped} ~ 70%n_{GR}. In the case of the q_{95} = 4.6 H-modes, Type I ELM frequency starts to decrease at n_{ped} ~ 60% n_{GR} possibly indicating a change in the ELM character at lower density than the low q H-modes. On the other hand, increasing the fuelling further does not increase the pedestal desnity significantly, and a transition to Type III ELMs occurs at $n_{ped} < 70\ n_{GR}$ or ~ 6.5 $10^{19} m^{-3}$.

These observations are summarised in Figs. 4 and 5 (open symbols for Type III ELMs) showing the difference in the pedestal parameters and confinement between low and high q_{95} H-modes. QDN plasmas at high q_{95} show a similar behaviour to the SN discharges: access to mixed type I-II ELM regime is essentially precluded in these conditions, with the transition to Type III ELMs taking place at low n_{ped}.

2.2 TYPE II ELM CHARACTERISATION

An interpretation of the change of ELM behaviour at high density (and increased inter-ELM losses, see paragraph 2.3) comes from the analysis of magnetic and density fluctuations. As already shown in [19] and [2], Type II ELMs in JET are accompanied by an increase of the intensity of broadband magnetic fluctuations at low frequency, associated with the changes in the pedestal and ELM behaviour described above. These broadband MHD events are called in JET washboard modes, or *W B* modes. As studied in detail in [13], there are strong indications that the presence of these modes has a “regulating” effect on the pedestal pressure and may be responsible for enhanced transport across the separatrix. In other words, increasing intensity of *W B* modes (ubiquitous in the edge of Type I ELMy H-modes in JET, [22]) may be associated with enhanced energy and particle losses between Type I ELMs ([13], [9]).

Figure 7 compares the MHD fluctuation intensity for four representative discharges in this study: two SN (HT 3) at q_{95} = 3.6 with type I and mixed Type I-II ELMs (Pulse No: 57897 and Pulse No: 57987), SN vs. QDN1, at the same I_p and B_T, both with mixed Type I-II ELMs (Pulse No: 57987 and Pulse No: 59237, time traces in Fig. 3) and last, low q_{95} vs. high q_{95} in SN at high n (Pulse No: 57987 and Pulse No: 58111). Fig.7(a) illustrates the typical change in MHD activity in the periods

between Type I ELMs, at low and high pedestal density (pulses 57897 and 57987) and the appearance of Type II ELMs "signature". The intensity of the MHD activity decreases at high frequency (>40kHz), while it is enhanced around the 20kHz level (±10kz). This is clearly visible in the spectrograms for these two same pulses (Figs. 8(a) and (b)), which also show the reduction in the type I ELM frequency in the presence of the enhanced inter-ELM MHD activity. Figure 7(b) shows that the *W B* mode signature for mixed Type I-II ELMs in SN and QDN is quite similar, with the fluctuations having similar intensity and frequency distribution for both configurations (see also Fig.8(b) and (c), middle and right plots). Finally, Fig.7(c) compares the *W B* mode intensity for two SN discharges at different q_{95}. Although a reduction of the high frequency MHD fluctuations is observed in both plasmas, at high q_{95} the characteristic intensity enhancement in the 20kHz range is absent or strongly reduced compared to the low q_{95} cases. The reason for this difference is not, at this moment, understood, but it is obvious that increasing the edge q does not seem to facilitate the access to the mixed Type I-II regime in JET, and even less an opening to total type I ELM suppression and steady Type II ELM H-mode edge. Increasing q_{95} in QDN configuration leads to similar results that for SN: at q_{95} = 4.1 in the QDN1 shape no clear Type II ELM phases are observed, for the investigated fuelling rates and Δ_{sep}.

As mentioned above, the new experiments presented in this work confirm the previous analysis of mixed Type I-II ELMy H-mode plasmas in JET, in particular that the presence of enhanced MHD activity between ELMs corresponds to a clamping of the pedestal temperature rise between ELMs. In fact, after the ELM crash, T_{ped} rises on a short time scale, but then remains essentially constant until the next ELM[19] (n_{ped} does not reach steady state during the type II ELM phase). Type II ELM losses are discussed in more detail in the next section (section 2.3). The behaviour of the density in the pedestal region during Type II ELM phases has been further investigated. Fast (100kHz) interferometry measurements in the region of the top of the pedestal show that the increased broadband MHD activity corresponds to a similar increase in the density fluctuations, as illustrated in Fig.9 for pulses 57897 and 57987, both 2.5MA/2.7T, linking the increase of the *W B* mode intensity not only to a saturation of T_{ped}, but also to increased particle losses between Type I ELMs (see also [9]).

Density fluctuations were also measured with a multi-channel heterodyne reflectometer, with maximum cut-off density of 5.1 $10^{19}m^{-3}$. Fluctuations were compared at different positions in the pedestal region. It is found that fluctuation levels between ELMs near the separatrix are very similar for pure Type I and for mixed Type I-II plasmas. Density fluctuations were also compared for density cut-off layers in the region of the maximum ∇n region in the pedestal, for both Type I and mixed Type I-II cases. The position of the selected cut-off layer in the pedestal gradient region for both pulses is shown in Fig.10. The density profiles in figure 10 are from pulses 59354 and 59355, that were performed as exact repeats of the SN HT 3 Type I ELM Pulse No: 57897 and mixed Type I-II Pulse No: 57987 respectively, to obtain high resolution edge density profiles, missing in the original pulses. A lower cut-off density was selected for pulse 57897 than for 57987, to compare the density fluctuation levels in similar relative positions in the gradient region in both pulses. The

corresponding intensity of the density fluctuations between ELMs is shown in Fig.11. No significant difference in the frequency distribution of the fluctuations in the steep gradient region of the pedestal is observed, between pure Type I and mixed Type I-II ELMs (both for SN and QDN). In particular no enhanced broadband fluctuations are observed ~ 20kHz, in contrast to the observation from interferometry. Figure 11 also includes density fluctuation data for the QDN1 Pulse No: 59237, showing a very similar distribution of density fluctuations from the steep gradient region of the pedestal as the other two SN plasmas. The decrease in the absolute intensity of n fluctuations is possibly related to changes of ∇n, and not to changes in turbulence.

The comparison of density fluctuation measurements from interferometry and reflectometry provides some indications on the localisation of the edge turbulence. In fact, the interferometer chord used for providing the measurements in Fig.9 is vertical and going across the approximate position of the pedestal top and, as discussed above, the fluctuation spectrum from these measurements is very similar to that of MHD fluctuations (Fig.8(a) and (b)). On the other hand, the reflectometry measurements in the steep gradient region and near to the separatrix do not indicate any significant change in the fluctuation spectra between Type I and mixed Type I-II ELMs. These finding suggests that inter-ELM transport in mixed Type I-II H-modes may be enhanced by a perturbation located in a very narrow region of the pedestal, probably near to the pedestal top.

2.3 LOSSES IN THE MIXED TYPE I-II REGIME

More insight may be gained on the failure to achieve steady Type II ELM regimes in JET, by analysing the changes in the re-heat and particle refuelling rates with ELM type, configuration and q_{95}. The analysis of the rate of rise of the stored energy between type I ELMs shows that, in general, dW/dt is not a constant, even for constant average plasma conditions, with dW/dt varying from ELM to ELM, as well as in time, between two ELMs. For the high δ plasmas analysed in this paper, dW/dt may vary from ~ 10 to near 0 MJs^{-1} (the stored energy rise between ELMs may reach near-saturation in some low-frequency Type I ELMy H-modes). Nonetheless, it can be shown that a qualitative correlation between dW/dt and the intensity of *W B* mode amplitude exists, in a similar way as what reported for the variation of the time evolution of T_{ped} between ELMs, [13].

In spite of the ELM-to-ELM variation of dW/dt, it is found that Type II ELMs phases correlate with a reduction of the power carried by Type I ELMs, P_{ELM}. With mixed Type I-II ELMs, the power carried by Type I ELMs is reduced by more than a factor of 2, as exemplified in Fig.12, left, comparing the re-heat rate of an HT3 Type I ELMy H-mode with that of a QDN1 with mixed Type I-II ELMs.

The right-hand side plot in Fig.12 shows the calculated fraction of power carried by Type I ELMs, P_{ELM}, (normalised to P_{sep}) for several 2.5MA/2.7T plasmas, with different magnetic configurations. The Fig. shows clearly that P_{ELM} is reduced from a maximum of 50 - 60% with Type I ELMs, down to ~ 25% in SN plasmas with mixed Type I-II ELMs and further down to ~ 20% for QDN1 with mixed Type I-II edge (or, in other words, ~ 80% of the power is exhausted across the separatrix in a quasi-continuous way). Nonetheless, the pedestal pressure is still evolving in the

Type II phases, indicating that these additional losses are not sufficient to avoid Type I ELMs completely. In particular, although the edge particle refuelling rate in Type II ELM phases is reduced by a factor ~ 2 compared to pure Type I ELM plasmas (Fig.13), dn/dt is still > 0. The plot to the left side of Fig.13 also shows that the net particle refuelling rate increases with q_{95}, with dn/dt at high q_{95} being a factor 1.4 to 1.8 higher than at lower q_{95}, for similar external gas fuelling. This, not surprisingly, results in a correlation between the higher refuelling rate and type I ELM frequency (Fig.13, right-hand side plot), although the reason why high q_{95} should result in a better effective particle confinement in the edge is not, to date, understood. This change in edge particle transport and the consequent increase of f_{ELM} may partially explain the reduced occurrence of Type II ELMs phases at high q_{95} in JET.

2.4 ASDEX-UPGRADE/JET TYPE II SIMILARITY EXPERIMENTS

The role of plasma magnetic geometry in accessing steady state Type II ELMy H-modes was further examined in a dimensionless identity experiment between ASDEX-Upgrade and JET, as outlined in paragraph 1.1. Two ideas were behind running dimensionless identical plasmas in the two devices: the first was to experimentally test QDN plasmas with the same δ and κ (JET QDN plasmas described in the previous paragraphs are more triangular and elongated than those in ASDEX-Upgrade) and Δ_{sep}, the second was to "use" the dimensionless identity to discriminate between Type II ELM access being determined by general plasma physics properties (that should be maintained in a dimensionless identity) or by other phenomena, such as atomic physics (changes in recycling and neutral penetration in the upper x-point region, for instance).

The model pulse from ASDEX-Upgrade was a 1MA/2.4T QDN H-mode plasma (q_{95} ~ 4.1), with H_{98} ~ 0.9, T_{ped} ~ 350eV and n_{ped} ~ 6.5 $10^{19}m^{-3}$ and steady Type II ELMy edge. Applying standard dimensionless identity relations (see, for instance, [3] and references therein), these parameters correspond in JET to 0.87MA/1.17T, with expected T_{ped} ~ 260eV and n_{ped} ~ 2.1 $10^{19}m^{-3}$, to match a pedestal collisionality ν^* ~ 2 and normalised toroidal Larmor radius ρ^* ~ 4 10^{-3}. The plasma average δ and κ were also matched, as indicated in Table 1 for the configuration QDN-sim.

The results of the experiments in identity conditions may be summarised as follow: long phases of H-mode confinement with no Type I ELMs, MHD signature consistent with Type II ELM activity and steady state pedestal parameters were observed, with H_{98} ~ 1 and pedestal densities n_{ped} ~ 85%n_{GR}. The duration of the period at constant pedestal parameters was limited by plasma core instabilities since, at these low input powers, the core plasma suffered from progressive density peaking leading to radiative collapse of the pulse. When either the input power or the plasma current and field (in steps up to 1.5MA/2.0T at constant q_{95} ~ 4.1) were increased, ELM activity typical of standard ELMy H-modes reappeared, and no ELM-free phases with constant pedestal parameters were obtained.

These findings are illustrated in more detail in Fig.14, showing selected time traces of two plasma discharges at 0.87MA/1.17T (pulse 62428 in red, and 62430 in blue). After a very similar

initial H-mode transition and long ELM free phase, the NB power was stepped up at about 24s in Pulse No: 62428 by ~ 1MW, while it was kept constant for 1s longer in Pulse No: 62430. The power increase in Pulse No: 62428 has two clear effects: T_{ped} increases and the pedestal goes into a standard Type I ELM phase; at the same time, the average plasma density (and core radiation) levels off and the plasma reaches stationary conditions. In contrast, the delayed power step up in Pulse No: 62430 corresponds to a short Type III ELM phase followed by ~ 1.5s (or ~ $4\tau_E$) period with approximately constant n_{ped} and T_{ped} and no Type I ELMs. The continuous rise in the core radiation keeps the power across the separatrix below that of Pulse No: 62428, even after the power is increased to the same level of Pulse No: 62428, and the pedestal temperature remains ~ 250eV (T_{ped} ~ 320eV for Pulse No: 62428). A close examination of the H_α traces both in the divertor and at the plasma outer midplane for Pulse No: 62430 shows that the typical bursts correlated to Type I ELMs are essentially absent, and only small and irregular oscillations are detected, which is similar to previous observations in Type II ELM phases of JET mixed Type I-II ELMy H-modes. As characteristic of Type II ELMs, an increase of magnetic turbulence (Fig.15) is observed during the quiescent phase of Pulse No: 62430, and it is identified as washboard modes, given their broadband characteristics, their frequency and the direction of rotation ([13] and [23]). The Type II ELM phase is terminated by the collapse of the plasma core.

Is interesting to note that, in the Type II ELM phase of Pulse No: 62430, the pedestal parameters of the JET discharge are very near to those expected from the identity calculations. In particular, the high value of pedestal collisionality of the ASDEX-Upgrade model pulse, ν^* ~ 2 is obtained. It appears that, in these identity conditions, the additional loss mechanism correlated to *W B* modes is sufficient to stabilise the pedestal density rise and both T_{ped} and n_{ped} are constant in time. These are, to date, the only conditions in JET where the increase in WB mode intensity (increased continuos power losses) is sufficient to reach steady state pedestal density. On the other hand, the power flux carried by Type II ELMs in these conditions is limited, as demonstrated by the pedestal behaviour of Pulse No: 62428: a small increase of P_{sep} (and decreased ν^*) results in a standard Type I ELMy edge. A detailed comparison of the MHD spectra for ASDEX-Upgrade and JET Type II ELMs is found in [23].

Finally, the operational space for achieving a Type II ELMy edge was further explored by increasing I_p/B_T at constant q. At both 1.2MA/1.6T and 1.5MA/2.0T a fine power scan was carried out to obtain again a steady Type II ELM edge, and at the same stable core profiles. Although phases of mixed Type I-II ELMs were obtained at 1.2MA, for the conditions explored the combination of I_p - B_T - P_{sep} resulting in the steady Type II phase of Pulse No: 62430 seems unique: at any power above the L $\rightarrow$ H power threshold, complete suppression of ELMs was not obtained (see Fig.16), indicating that the operational space for Type II ELMs may close down when the minimum power to obtain an H-mode increases because B_T is increased, possibly related to the increase of the minimum T_{ped} ($T_{ped} \propto B_T^{0.8}$, [1]) required to sustain an H-mode.

3. SMALL ELM REGIMES AT HIGH β_p

This section describes the behaviour of the pedestal and ELMs in high β_p H-mode plasmas. As outlined in paragraph 1.1, the possible effect of β_p on ELM behaviour was investigated by carrying out a β_p scan in ELMy H-modes, in a QDN configuration. The experiments were carried out in plasmas with a fully penetrated current profile and no ITB, with $l_i > 1$ for $\beta_p > 1.3$. The plasma shape was QDN, with $\Delta_{sep} \sim 1$cm (high l_i high β_p configuration, $\delta \sim 0.45$, table 1). In this experiment, β_p was increased in steps from 1.1 to 1.9, by increasing the input power (combined NB and H minority central ICRH) and, at the maximum input power, reducing the plasma current at fixed field. In particular, the toroidal field was fixed at BT = 2.7T to optimise fast ECE profile measurements, and the plasma current varied from 1.5 to 1.35 and finally down to 1.2MA. In this scan, q_{95} varied from ~ 5 to ~ 7, with the highest q_{95} corresponding to the discharges with the highest β_p. Total input power, β_p and edge safety factor q_{95} for 7 representative discharges of the series are shown in Fig.17, while the corresponding divertor H_α traces (enlarged for clarity) are in Fig.18.

At lower input powers, up to $\beta_p \sim 1.5$, the ELM H_α signature is typical of a Type I ELMy H-mode edge: distinct spikes with frequency increasing with input power. At $\beta_p \sim 1.65$ (Pulse No: 62409 at 1.2MA/2.7T, $q_{95} \sim 6.5$), a change in the ELM activity is observed, with long phases where the H_α spikes disappear at constant plasma confinement. When β_p is increased further ($\beta_p \sim 1.8$ - 1.9), regular ELM activity is no longer detectable in the divertor H_α signature: type I ELM completely disappeared to be replaced by high frequency, very small and irregular oscillations, strongly reminiscent of the grassy ELMs of JT-60U, [7]. This change in the ELM behaviour occurs at high confinement ($H_{98} \sim 1.0$ - 1.2) and high density ($n \sim 85\% n_{GR}$). Both pedestal and core profiles are in steady state: edge losses associated to these small ELMs are clearly sufficient to carry all the power and particles normally lost by Type I ELMs. Moreover, grassy ELMs are compatible with high global confinement with the highest confinement ($H_{98} \sim 1.2$) obtained at the highest β_p. Changes in the MHD fluctuation pattern accompanying the change in the ELM H_α signature, as shown in Figs. 19 for Pulse No: 62406 (Type I ELMs, $\beta_p \sim 1.35$) and 20, for Pulse No: 62413 ("grassy" ELMs, $\beta_p \sim 1.9$). Although fast magnetic measurements are available up to 1MHz frequency, the figures include only fluctuations in the 0 - 50kHz range, to make the features of the Grassy ELMs MHD visible. The comparison of the two MHD spectrogrammes shows that small MHD bursts are still associated with Grassy ELM activity, in a way that is reminiscent of the standard MHD signature of Type I ELMs, although the extent in frequency of the MHD perturbation is dramatically reduced compared to Type I ELMs. In contrast to Type II ELMs, the typical 20kHz broadband magnetic turbulence is not observed in the grassy ELM discharges and, in fact, the the regime seems to be characterised by a very low level of MHD fluctuations for frequencies between 10kHz and 1MHz.

To understand the reasons for the change in ELM behaviour at high β_p observed in the high l_i H-modes, these pulses were compared to standard ELMy H-modes at low β_p ($\beta_p < 1$) [11], as well as to a series of discharges carried out at 1.2MA/2.7T (like most of the high l_i H-modes), and where β_p was varied over a similar range, from ~ 1.1 to ~ 1.9. In this latter experiment, Lower Hybrid pre-heating

and early main heating was used to control the q profile, and resulted in plasmas with $q_0 > 2$ and broad current profile ($l_i \sim 0.85$), with some of these discharges having a weak ion ITB. The pulses in this series are identifies as "lowl_i-highβ_p" H-modes (see table 1). These plasmas are standard lower SN ($\Delta_{sep} \sim 4$cm), with the same δ, κ and similar q_{95} as the QDN used for the high l_i - high β_p H-modes. The time traces of total input power (also NB and ICRH combined heating, as for the high l_i H-modes), β_p and q_{95} are shown in Fig.21, while the corresponding divertor H_α traces are shown in Fig.22: in contrast to the previous case, increasing β_p does not cause a change in the ELM behaviour, and Type I ELMs are observed up to the highest β_p. Furthermore, MHD spectrogrammes show the typical type I ELM signatures, consistently with the H_α traces.

3.1 CONFINEMENT AND PEDESTAL CHARACTERISTICS OF HIGH β_p H-MODES

In this paragraph, the global plasma confinement and pedestal behaviour are analysed, to identify differences and similarities in the high β_p, high- and low l_i H-modes, that may explain the observed difference in ELM behaviour.

The global plasma confinement of the two series of high β_p is compared in Fig.23 , showing the confinement enhancement factor H_{98} as function of the normalised pedestal density $n_{ped}/\tilde{n}_{GR}$. At low β_p, the low l_i H-modes have reduced H_{98} compared to both standard Type I ELMy H modes of that density and high l_i H-modes ($H_{98} \sim 0.7$ - 0.9), but for $\beta_p > 1.5$, the global confinement of high- and low-l_i plasmas is very similar, with $H_{98} \sim 1.1$ - 1.2 in both cases.

The pedestal pressures of the two groups of high β_p plasmas are compared in Fig.24. Since some of the plasmas of the high-l_i series had $I_p \neq 1.2$, p_{ped} in Fig.24 is normalised, to allow a direct comparison of all the data (normalisation to I_p^2 [11], to 1.2MA). In the case of the high l_i H-modes, p_{ped} is essentially constant with β_p, indicating that the onset of the small and high-frequency grassy ELMs does not reduce the pedestal energy content, in contrast to what is observed at the Type I $\rightarrow$ Type III ELM transition [21]. For the low l_i H-modes, p_{ped} increases with β_p, consistently with the global plasma confinement behaviour and, for $\beta_p \sim 1.9$, p_{ped} is very similar to that of the high β_p high l_i H-modes. Figure 24 also shows a potentially important difference between the two groups of plasma pulses, namely that the pedestal of the high l_i H-modes is more collisional than that of the low l_i H-modes. In particular, this difference is the largest at high β_p: the high l_i plasmas with grassy ELMs have pedestal e-e collisionality $0.4 < \nu^* < 0.7$ for $1.7 < \beta_p < 1.9$, compared to that of the low l_i plasmas that, in the same range of β_p, have $\nu^* < 0.15$. This difference is due to operational reasons: all the high β_p high l_i H-mode have strong edge fuelling, to obtain pedestal densities in the range of $\nu^* < 70\% n_{GR}$. The fact that grassy ELMs are only observed above $\nu^* < 0.4$ therefore does not, in principle, represent an "existence limit" in ν^* for these ELMs, but only reflects the range of pedestal parameters investigated so far.

3.2 COMPARISON OF TYPE I AND "GRASSY" ELM LOSSES

The relevance of achieving a "grassy" ELM edge at high plasma confinement depends on the reduction of bursty ELM losses: in fact, although the H_α pattern would indicate that the grassy

ELMs are small, a quantitative evaluation of energy losses associated to the small and irregular H_α bursts is required to judge the value of this regime for future development.

Prompt ELM energy losses, temperature and density drop at ELMs were analysed for both high- and low l_i H-modes and compared to the existing JET database from standard ELMy H-modes (Type I and Type III, $\beta_p < 1$, [11]). The results of this analysis are summarised in Figs. 25(a),(b) and (c). Fig.25(a) shows the ELM energy losses ΔW_{ELM}, normalised to the pedestal energy W_{ped}; Fig.25(b) shows, for the same set of pulses, the pedestal electron temperature drop at the ELM, ΔT_{ELM}, normalised to $T_{e,\,ped}$ and, finally, Fig.25(c) shows the pedestal density drop at the ELM, $\Delta n_{e,\,ELM}$, normalised to the pedestal electron density n_e. Energy losses, temperature and density drop all give the same picture: the high l_i H-modes ELM losses are comparable to those of standard H-modes up to $\beta_p \sim 1.5$, that is when they exhibit a Type I ELM edge. At higher β_p, the energy loss associated with "grassy" ELMs is very small, below detection limit (~ 50kJ), and corresponding to a maximum of $\delta W_{ELM} / W_{ped} \sim 4$ - 5%. These losses below detection limit are represented by the red bars, where the top of the bar represents the maximum estimated loss. The low energy losses with grassy ELMs are confirmed by the analysis of $T_{e,\,ped}$ and $n_{e,\,ped}$ drops. Note that the high resolution of the ECE and of the interferometer used for this analysis allow to resolve ELMs δT and δn that are too small for the fast stored energy loss measurements. Figures 25(b) and 25(c) show that both temperature and density drop for grassy ELMs are below those of Type I ELMs with similar ν^*, and even lower than those measured for Type III ELMs, in spite of the global confinement and pedestal pressures with grassy ELMs being similar or higher than expected for a type I ELMy H-mode. In contrast, ELM losses of the low l_i H modes are similar to those of standard Type I ELMs, although the lack of data on the ELM density losses does not allow a more detailed comparison.

The reduction of the size of grassy ELMs compared to Type I ELMs may be explained by comparing the ELM affected depth, L_{ELM}. L_{ELM} is estimated from the radial extent of the prompt perturbation of the radial T_e profile caused by an ELM. The perturbed T_e profile is obtained by subtracting the post-ELM T_e profile from the pre-ELM T_e profile, dividing the difference profile to the initial $T_e(r)$ and then normalising it to its maximum.

Figures 26(a) and (b) compare L_{ELM} for two groups of data: Fig.26(a) shows the perturbed T_e profiles for a density scan in standard H-modes (at fixed I_p/B_T, shape and P_{in}), including both type I and Type III ELMs; although increasing the density (ν^*) reduces ELM losses by factor ~ 3 (or ~ 2 when normalised to W_{ped}), the ELM affected depth does not change significantly as long as the pedestal maintains Type I ELMs. Fig 26(b) compares L_{ELM} for ELMs from two plasmas in the HT3 configuration at low and medium q_{95} (~ 3.6 and ~ 4.5, from the same series of pulses described in paragraph 2.1) and shows that, although increasing q_{95} from ~ 3.6 to ~ 4.5 reduces Type I ELM losses very significantly (by a factor of 3 - 4), L_{ELM} again remains the same. A reduction of ELM size accompanied by a reduction of the ELM affected depth is observed only in the case of Type III ELMs (Fig.26(a), open symbols), that is for ELMs that are probably caused by a different MHD instability than Type I ELMs, [11]. These observations can be contrasted with the behaviour of

L_{ELM} in the high l_i H-mode β_p scan, shown in Fig.26(c). In this case, one see that the reduction of the ELM losses observed with grassy ELMs at high β_p corresponds to a shrinking of the ELM affected depth, strongly suggesting that a change in the MHD instability or consequent relaxation in the pedestal may be at the root of the reduction in the ELM size. Such a reduction of L_{ELM} with β_p is not observed for the low l_i H-modes, which are similar in this regard to standard H-modes, as may be expected, since they maintain a Type I ELMy pedestal.

4. DISCUSSION

As shown in section 2, a steady state H-mode with a Type II ELMs and complete Type I ELM suppression has not been achieved in JET, so far, for the normal JET plasma operating conditions (medium current I_P ~ 2 - 3MA, q_{95} ~ 3 - 3.6). However, at high shaping and density, mixed phases of Type I-II ELMs are observed regularly and reproducibly in these conditions, both in SN and QDN plasmas. It has been shown that, in contrast to indications from other experiments, increasing q_{95} both in SN and QDN, from ~ 3 to ~ 4.5 (by varying either I_p or B_T), does not facilitate the access to the Type II ELM regime (paragraph 2.1). Moreover, increasing q_{95} affects the pedestal behaviour in the Type I ELM regime: the Type I ELMs frequency is much higher than at q_{95} ~ 3, no clear Type II ELM phases are detected, and Type I-III ELM transitions occur at lower pedestal density than at lower q_{95}.

The interpretation of these results in terms of changes of the ideal MHD stability of the pedestal is not straightforward and unequivocal. In [12] an MHD ELM model is put forward to interpret the changes in ELM type observed in experiments for increasing density, variation of the edge safety factor, β_p and shape. In this model, Type I ELMs occur when the pedestal is in the second stability region (to $n = \infty$ ballooning modes), and are caused by the pedestal gradients reaching a finite-n ballooning stability limit. In contrast, Type II ELMs are assumed to originate from a different MHD instability, namely ideal $n = \infty$ ballooning modes. Mixed Type I-II regimes are interpreted as being the result of different zones of the pedestal being dominated by a different instabilities: the inner part of the pedestal region is in the second stability regime, and large perturbations (Type I ELMs) occur when the finite-n ballooning limit is reached, while the outer part of the pedestal is instead $n = \infty$ ballooning unstable (and limited to a lower critical pressure gradient), and smaller and more frequent ELMs (Type II) are therefore generated when this limit is reached. This model has been applied to the comparison of MHD stability of high δ, high κ SN and QDN plasmas both in predictive and interpretative simulations (using experimental profiles from discharges with the same I_p, B_T and input power) with the JETTO - MISHKA suite of codes . It is found that the variation of the magnetic geometry from SN to QDN does not change the MHD stability of the pedestal in a qualitative way, and the access to the mixed Type I-II regime is similar in both cases. The experimental fact that plasmas with QDN magnetic geometry tend to reach higher n_{ped} than similar SN plasmas has a stronger effect on the access to the Type I-II regime that magnetic geometry alone. These results are in qualitative agreement with the experimental findings reported in this paper, in particular with the observations that the longest Type II ELM periods are observed in QDN plasmas, as well

as the largest increase in inter-ELM losses is the mixed Type I-II regime (see Fig.12(b)). In contrast, MHD stability analysis of the ASDEX-Upgrade Type II ELMy H-modes, carried out with the IDBALL and GATO codes [16], showed that the combination of proximity to Double Null and high q_{95} has a clear effect on the pedestal stability. In particular, approaching Double Null configuration, at high desnity and q_{95}, has the effect of stabilising low-n peeling/ballooning modes and to increase the localisation of the modes in the edge region. This is found to be in qualitative agreement with the change from Type I to Type II ELMs observed in ASDEX-Upgrade in those experimental conditions.

The ELM model in [12] was also applied to the study of the effects of q_{95} on pedestal and ELM stability. The simulations find that increasing q_{95} increases the magnetic shear in the edge, as well as changing the $n = \infty$ ballooning stability limits in the edge region, and the combination of these two effects is indeed favorable to the onset of Type II ELMs. Although this modelling result is consistent with findings from other devices, it does not reflect the experimental observations for JET plasmas. The observed variation of Type I ELM size and frequency with q_{95} is analysed by [17], for the case of JET pulses of fixed shape (medium δ) and varying q_{95}: in this case it is found that the the dominant instabilities are low to intermediate n peeling-ballooning modes, and that increasing q_{95} "moves" this limit to higher values of the normalised pressure gradient (and to higher values of the pressure gradient itself). Interestingly, increasing q_{95} has very little effect on the radial extent of the most unstable modes, indicating that the change in ELM frequency and size is not due to a change in the structure of the triggering instability.

H-modes with pure Type II ELM edge and constant n_{ped} and T_{ped} were indeed obtained in JET/ ASDEX-Upgrade Type II ELM identity conditions. Unfortunately, since these experiments were carried out a low I_p, the quality of the edge profile measurement is not sufficient for a meaningful MHD stability analysis; nonetheless, these experiments may give some indications on possible physics mechanisms of Type II ELMs. In particular, the observation that any increase in input power and/or current and field results in Type I and Type III ELMy H-mode edge suggests that the amount of power and particle exhaust carried by "continuous" transport due to the Type II ELMs is limited, with this loss mechanism possibly being associated to low pedestal temperature or high collisionality regimes (see [13], [23]). Transport simulations were carried out of the JET/ASDEX-Upgrade identity Pulse No: 52430, where long Type II ELM phases were found and compared to simulations of other discharges in the same series, where Type I ELMs were still observed. For these particular conditions, transport analysis would indicate that neoclassical losses could play an important role for the pedestal to reach steady state before reaching the Type I ELM MHD limit.

The most successful scenario to date for obtaining small ELMs and simultaneous high pedestal pressure and confinement in steady state in JET is the combination of high shaping (in this case QDN), high β_p ($\beta_p > 1.65$) and high q_{95}. There are several similarities in the phenomenology of the grassy ELMy H-modes in JET and in JT-60U, in particular the existence of a threshold value for the global β_p for the onset of these ELMs. On the other hand, the comparison of the ELM behaviour of

high-l_i and low-l_i H-modes at high β_p (section 3) would indicate that, for the case of JET, high β_p is possibly a necessary but not sufficient condition for obtaining a grassy ELMy H-mode edge. One possible explanation for the change in ELM character at high β_p, put forward for the JT-60U grassy ELM plasmas, [7] and [8], is that grassy ELMs are the result of a change in the ideal MHD stability of the pedestal, caused by the compression of the magnetic surfaces in the edge due strong Shafranov shift (Δ_S). This mechanism for the change in the peeling-ballooning stability of the pedestal is also put forward by [15], in combination with high δ effects, for the interpretation of the effect of high β_p on pedestal and ELMs in ASDEX-Upgrade pulses.

In the case of the high β_p experiments in JET, Δ_S for both high- and low-l_i H-modes is shown in Fig. 27, as function of β_p. Δ_S is quite high in both cases, reaching values ~22 - 26% of the minor radius for $\beta_p > 1.7$. Nonetheless, grassy ELMs are observed only for the high l_i H-modes. This observation suggests that other factors contribute to the change in stability of the pedestal at high β_p: one possible contribution may come from the differences in the current profiles of the two groups of high β_p pulses, as illustrated in Fig.28. Grassy ELMs are observed at high β_p in pulses with a rather peaked current profile ($l_i > 1.1$), compared to the companion plasmas at the same β_p but with broader current profile ($l_i < 0.85$), at the same total plasma current. One may speculate that the contribution of the inductive current to the edge current will be smaller in case of high l_i, reducing the total amount of toroidal current in the edge and therefore improving the pedestal stability against low- medium-n peeling-ballooning modes (this mechanism is invoked by [15] in the case of high β_p H-modes in ASDEX-Upgrade). It is interesting to note that both [15] and [12] find that increasing β_p changes the stability of the pedestal towards a more ballooning type of instability, although the two authors identify different specific instability triggering the Type II ELMs (high-n ballooning in [15] and n = ∞ ballooning in [12]).

5. CONCLUSIONS AND OUTLOOK

The access to ELMy H-modes with high confinement and small ELMs has been investigated in detail in JET. It is found that, in standard plasma conditions (I_P ~ 2 - 3MA, q_{95} ~ 3 - 3.6), high shaping ($\delta > 0.4$) and high pedestal density ($n_{ped} > 70\% n_{GR}$), the pedestal accesses a mixed type I-II ELM regime. This regime is observed for both SN and QDN magnetic configurations. Long periods of Type II ELMs (up to 150ms in QDN) are obtained at high n_{ped}, associated with an increase of both magnetic and density fluctuations, compared to levels in Type I ELMy H-modes. Measurements of density fluctuations by interferometry and reflectometry indicate that the location of these enhanced fluctuation region is likely to be near the pedestal top. Increasing q_{95} from ~ 3 to ~ 4.5 (by varying either I_p or B_T at constant plasma shape), does not facilitate the access to the Type II ELM regime, in contrast to indications from other experiments. The enhanced ~ 20kHz magnetic fluctuations observed in the Type II ELM periods are identified as strong washboard modes, possible responsible for the increased inter-ELM transport. Power balance calculations do indeed show that the power carried by Type I ELMs is reduced by more than a factor of 2 to 3 in the presence of enhanced MHD

between ELMs, with P_{ELM}/P_{sep} going from a maximum of 50%-60% in Type I ELM discharges, down to 27% in SN plasmas and to 21% in QDN. Evaluation of the inter-ELM refuelling rate shows that enhanced particle losses associated with type II ELMs are nonetheless insufficient to drive the pedestal to steady state. This would indicate that control of the density rise rate at the plasma edge may be crucial for achieving steady state Type II ELMs at high confinement, in particular for plasmas near to Double Null (T_{ped} saturates between ELMs). In JET (and ITER), the long absolute particle confinement time may necessitate active control of recycling in the upper x-point region as well as of fluxes from the main chamber/limiters.

The role of QDN magnetic geometry, in achieving Type II ELMs in steady state, was further investigated in JET/ASDEX-Upgrade identity experiments (0.87MA/1.17T , $q_{95} \sim 4.1$ and $P_{in} \sim 4$MW). For the first time, long Type II ELM phase, with constant n_{ped} and T_{ped} were obtained with the pedestal parameters matching the identity conditions (in particular, $\nu^* \sim 2$) with the Type II ELM periods being terminated only by core radiative collapse. Strong washboard mode activity is observed during the Type II ELM periods, similar to that of the higher current mixed Type I-II plasmas described above. Increasing P_{in} at fixed plasma parameters results in the reappearance of type I ELMs, indicating that the amount of power/particles that can be exhausted across the separatrix by Type II ELMs in these conditions is rather small. Similar results are found by increasing I_p/B_T at constant q: as soon as enough power was applied to obtain a H-mode, standard Type III or Type I ELMs reappear. Even with QDN, high ν^* and/or low T_{ped} (resistive MHD) may be required to obtain Type II ELMs and sufficient losses to maintain the pedestal in steady state, casting doubts on the potential for extrapolation of this ELM regime to hot plasmas.

The investigation of the effect of high β_p on the pedestal and ELM in H-mode plasmas has shown that small and irregular ELMs (Grassy ELMs) appear above $\beta_p > 1.6$-1.7, in high l_i H-modes. Grassy ELMs cause very low bursty energy and particle losses, smaller than those measured for Type I ELMs at the same collisionality, pedestal pressure and global confinement, but sufficient to obtain steady state in the plasma pedestal and core. Analysis of the fast perturbation of temperature profile at the ELM shows that the reduction of ELM losses with grassy ELMs may be attributed to the shrinking of the ELM affected depth. This finding (in contrast to the case of Type I ELMs, where changes in ELM amplitude occur at constant L_{ELM}) suggests that the onset of grassy ELMs may be due to a change in the mode(s) making the pedestal MHD unstable. Comparison between low- and high-l_i H-modes indicates that high β_p is a necessary but not sufficient condition for obtaining grassy ELMs.

The operational space for grassy ELMs in JET needs to be explored further and extended, to establish the relevance of this small ELM regime as an ELM mitigation scenario. The conditions of the experiments described in this paper are such that all the high β_p pulses with grassy ELMs were obtained in plasmas with extremely high safety factor ($q_{95} \sim 6.5$ - 7) and relatively high pedestal collisionality (minimum $\nu^* \sim 0.4$), although these values of q_{95} and ν^* were dictated by experimental constraints (available input power, range of density explored) and do not represent, in principle, an

existence boundary for grassy ELMs onset. Moreover, a QDN configuration was used for the high-l_i experiments, as opposed to the SN used for the low l_i H-modes, leaving open the question of the role of magnetic geometry in obtaining this small ELM regime. Future experiments should focus on obtaining high β_p plasmas at lower ν^* and q_{95}. In those conditions, the systematic investigation of the role of edge currents and plasma shape in determining the operational space of grassy ELMs would also be required, to clarify the extrapolation potential of this regime.

ACKNOWLEDGEMENTS

The authors thank all the JET-EFDA collaborators for the help in the execution of the experimental programme and in the data analysis. The experiments described in this paper were carried out in the JET-EFDA Task Force S1 in 2002-2003. The efforts of all members of the Task Force, and of the Task Force Leaders in the organisation of the experiments, data analysis and publication of results are gratefully acknowledged.

REFERENCES

[1]. Y. Andrew, N.C. Hawkes, M.G. O'Mullane, et al. (2004). Plasma Phys Control Fusion **46**, 337.

[2]. M. Becoulet, B. Alper, S. Gerasimov, et al. (2001). Edge Fast Magnetics Measurements During ELMs of Different Types in JET. submitted to Plasma Phys Control Fusion, special issue Proc of IAEA TCM on Divertor Concepts, Aix en Provence (France), 2001.

[3]. J.G. Cordey, B. Balet, D. Campbell, et al. (1996). Plasma Phys Control Fusion **38**, A67.

[4]. T.E. Evans, R.A. Moyer, P.R. Thomas, et al. (2004). Phys Rev Lett **92**, 235003.

[5]. G. Federici, P. Andrew, G. Barabaschi, et al. (2003). Jour Nucl Mater **313- 316**, 11.

[6]. M. Greenwald, M. Bell, S. Ejima, et al. (1988). Nuclear Fusion **28**, 2199.

[7]. Y. Kamada, H. Tanekaga, A. Isayama, et al. (2002). Plasma Phys Control Fusion **44**, A279.

[8]. Y. Kamada and the JT-60U Team (2001). Nuclear Fusion **41**, 1311.

[9]. H.R. Koslowski, C.P. Perez, G.D. Conway, et al. (2003). Relation Between Type-II ELMs, Edge Localized Turbulence, Washboard Modes and Energy Losses Between ELMs in High Density ELMy H-Modes on JET. 30th EPS Conference on Contr. Fusion and Plasma Phys., St. Petersburg, 7-11 July 2003 ECA Vol. 27A, P-1.102.

[10]. P.T. Lang, J. Neuhauser, L.D. Horton, et al. (2003). Nucl Fusion **43**, 1110.

[11]. A. Loarte, G. Saibene, R. Sartori, et al. (2004). Phys of Plasmas **11**, 2668.

[12]. J.-S. Lonnroth, V. Parail, G. Huysmans, et al. (2004). Plasma Phys Control Fusion **46**, 767.

[13]. C.P. Perez, H.R. Koslowski, T.C. Hender, et al. (2004). Plasma Phys Control Fusion **46**, 61.

[14]. F. Ryter, J. Stober, A. Stabler, et al. (2001). Nuclear Fusion **41**, 537.

[15]. S. Saarelma and S. Guenter (2004). Plasma Phys Control Fusion **46**, 1259.

[16]. S. Saarelma, S. Guenter, L.D. Horton, et al. (2003). Nucl Fusion **43**, 262.

[17]. S. Saarelma, V. Parail, E. de la Luna, et al. (2004). MHD Stability Analysis of Diagnostic Optimized Configuration (DOC) Shots in JET. submitted to Plasma Phys Control Fusion.

[18]. G. Saibene, P. J. Lomas, M. Becoulet, et al. (2001). The Effect of Plasma Shape on Density and Confinement of ELMy H-Modes in JET. Proc 28th Conf on Controlled Fusion and Plasma Physics, Madeira (PT) - paper P3.002/Or.28.

[19]. G. Saibene, R. Sartori, A. Loarte, et al. (2002). Plasma Phys Control Fusion **44**, 1769.

[20]. R. Sartori, P. Lomas, G. Saibene, et al. Scaling Study of ELMy H-Mode Global and Pedestal Confinement at High Triangulairty in JET. IAEA, Vienna. Proc of the 20th Fusion Energy Conf 2004, November 2004, paper IAEA-CN-116/EX/6-3.

[21]. R. Sartori, G. Saibene, L.D. Horton, et al. (2004). Plasma Phys Control Fusion **46**, 723.

[22]. P. Smeulders, G.D. Conway, B. Alper, et al. (1999). Plasma Phys Control Fusion **41**, 1303.

[23]. J. Stober, P. Lomas, G. Saibene, et al. Small ELM Regimes with Good Confinement on JET and Comparison to Those on ASDEX-Upgrade, Alcator C-mod, and JT-60U. IAEA - Vienna. Proc of the 20th Fusion Energy Conf 2004, November 2004, paper IAEA-CN-116/EX/P1-4.

[24]. J. Stober, M. Maraschek, G.D. Conway, et al. (2001). Nuclear Fusion **41**, 1123.

Conf	Name	I_p(MA)	B_T(T)	q_{95}	κ_{sep}	$\delta_{sep,average}$
SN	HT3	2.5	2.7 – 3.4	3.6 – 4.6	1.74	0.42
QDN	QDN1*	2.5 – 2.1 – 1.9	2.7	3 – 3.7 – 4.1	1.75 to 1.9*	0.43 to 0.50*
QDN	QDN-sim	0.87 – (1.2 – 1.5)	1.17 – (1.6 – 2.0)	4.1	1.7	0.35
QDN	highl_i - highβ_p	1.5→1.2	2.7	4.8→6.9	1.62	0.45
SN	lowl_i-highβ_p	1.2	2.7	6 – 7	1.62	0.45

JG05.44-1c

Table 1:

Summary of magnetic geometry and main plasma parameters of the configurations used in the small ELM experiments described in the text. All SN configuration have the second x-point outside the vacuum chamber, while for QDN configurations the second x-point is inside. These magnetic configurations are further described in terms of Δ_{sep}, the distance (mapped to the outer midplane) between fist and second separatrix. Several variants of the QDN configuration were used in the experiments, such as variations of Δ_{sep} in QDN1 (Δ_{sep} from ~ 2cm to $<$ 1cm), reduced δ and κ for QDN-sim and small modification of the divertor strike point position in the highl_i-highβ case. Note the $\Delta_{sep} > 4$cm for the SN configurations.

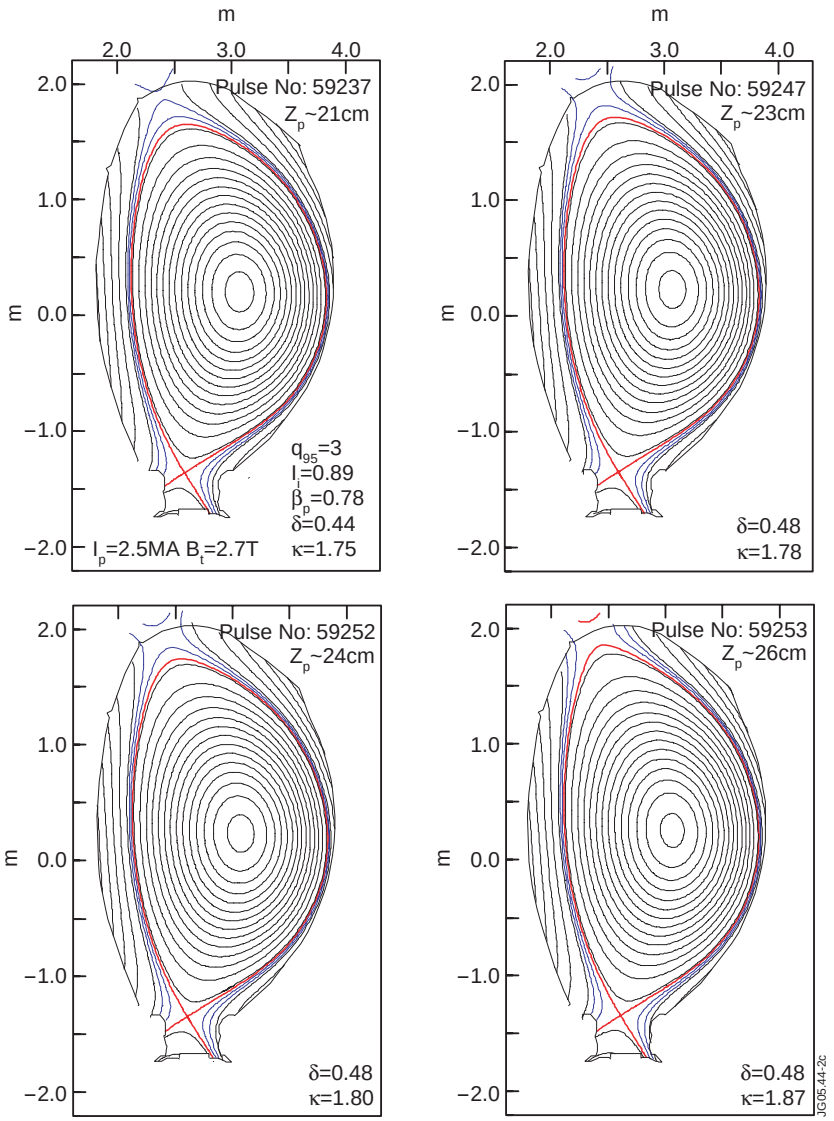

Figure 1: Equilibrium reconstruction of 4 plasma discharges used for the QDN proximity studies. The variation of Δ_{sep} from ~ 2cm to < 1cm is achieved by moving the plasma vertically upwards (as indicated by the variation of the centroid position Z_p shown for each case). The blue lines are the 1cm and 2cm midplane flux surfaces.

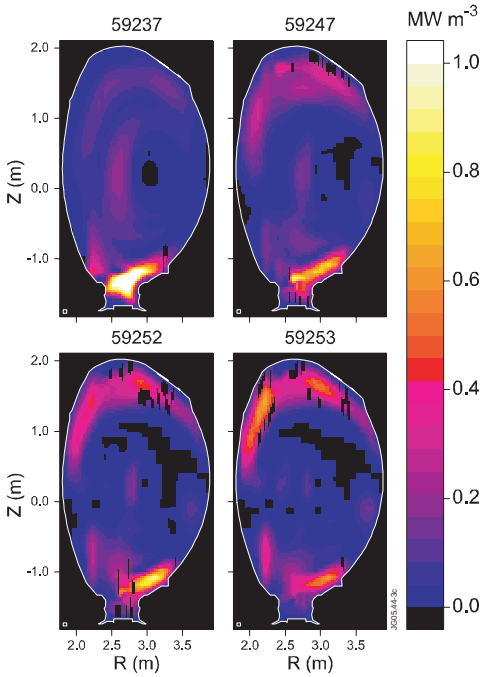

Figure 2: tomographic reconstruction of the poloidal distribution of the radiation emission for each of the 4 plasmas shown in Fig. 1.

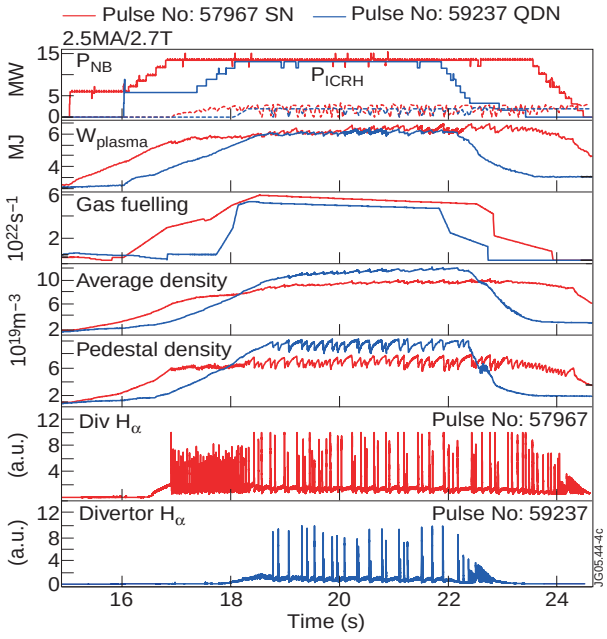

Figure 3: selected time traces of the SN HT3 Pulse No: 57987 (red traces) and of the QDN QDN1 Pulse No: 59237 (blue traces). Pulse No: 59237 is the QDN pulse that reached the highest plasma confinement (see also Fig. 5), and has comparable stored energy to similar single null pulses, and to Pulse No: 57987 in particular. I_p = 2.5MA and B_T = 2.7T for both pulses, with q_{95} = 3.6 and 3 respectively. Both Pulse No: 57987 (18 → 23s) and Pulse No: 59237 (19 → 22s)are in the mixed Type I-II regime. The traces in the graph are, top to bottom: NB (P_{NB}, MW) and ICRH (P_{ICRH}, MW) input powers; plasma stored energy (W_{plasma}, MJ); gas fuelling rate (10^{22} atoms s^{-1}); plasma average density ($10^{19} m^{-3}$); pedestal density ($10^{19} m^{-3}$) and, in the last two boxes, divertor H_α emission.

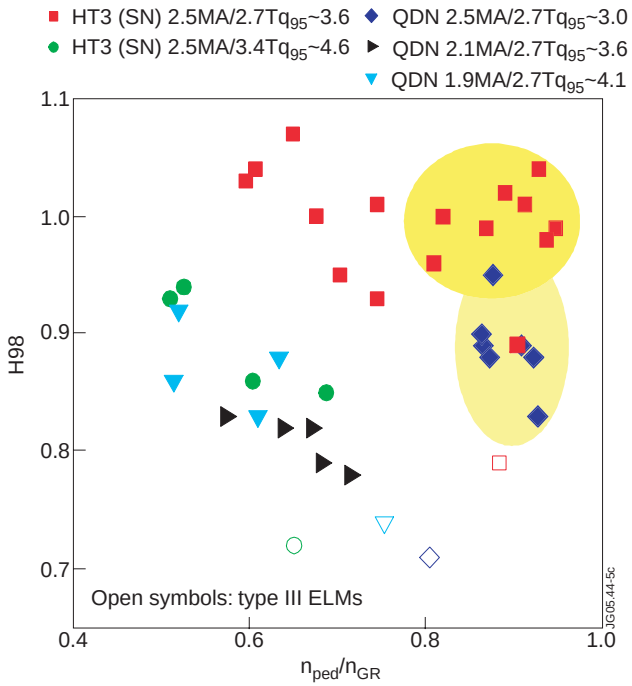

Figure 4: confinement enhancement factor H98 as function of normalised pedestal density nped/n_{GR}, for both HT3 and QDN1 plasmas, including the q_{95} scans.

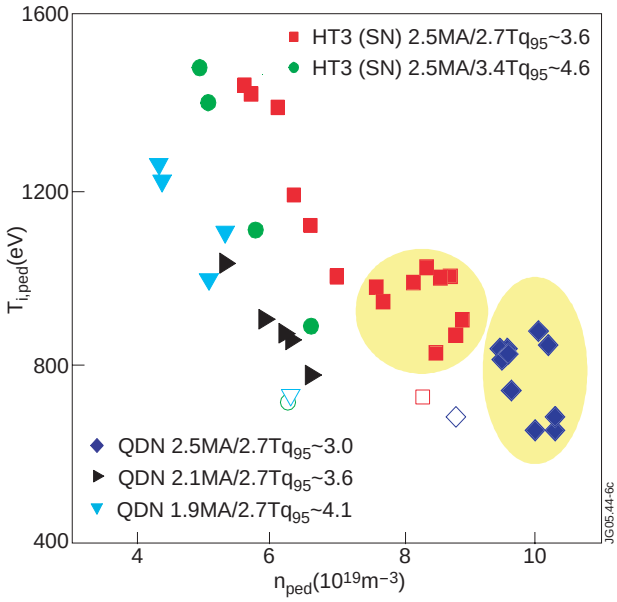

Figure 5: n_e - T_i diagram for the top of the pedestal of the same discharges as in Fig. 4. The legend for the symbols here is the same as for Fig. 4. T_i (from the edge charge-exchange spectroscopy system) is used instead of T_e because the latter is not available for all discharges due to ECE emission cut-off at high pedestal densities.

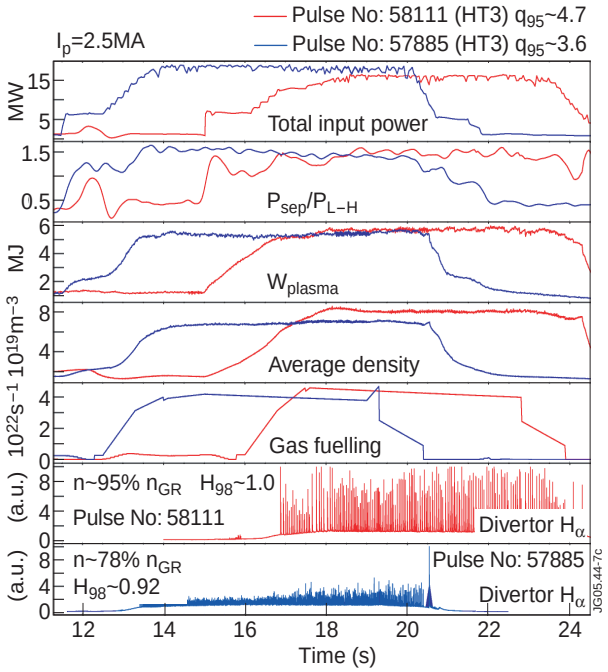

Figure 6: selected time traces for 2 SN HT 3 H-modes at 2.5MA: Pulse No: 57885 (red), with B_T = 2.7T and q_{95} ~ 3.6 and Pulse No: 58111 (blue), with B_T = 3.4T and q_{95} ~ 4.7. The time traces are, from top to bottom: total input power (P_{tot}, MW), ratio of the power across the separatrix P_{sep} to the H-mode power threshold P_{L-H} [Ryter et al., 2001] (P_{sep} = P_{tot} - P_{rad} - dW/dt), plasma stored energy (W_{plasma}, M J), plasma average density ($10^{19}m^{-3}$), gas fuelling (10^{22}atoms s^{-1}) and, last two boxes, divertor H_α emission, in arbitrary units.

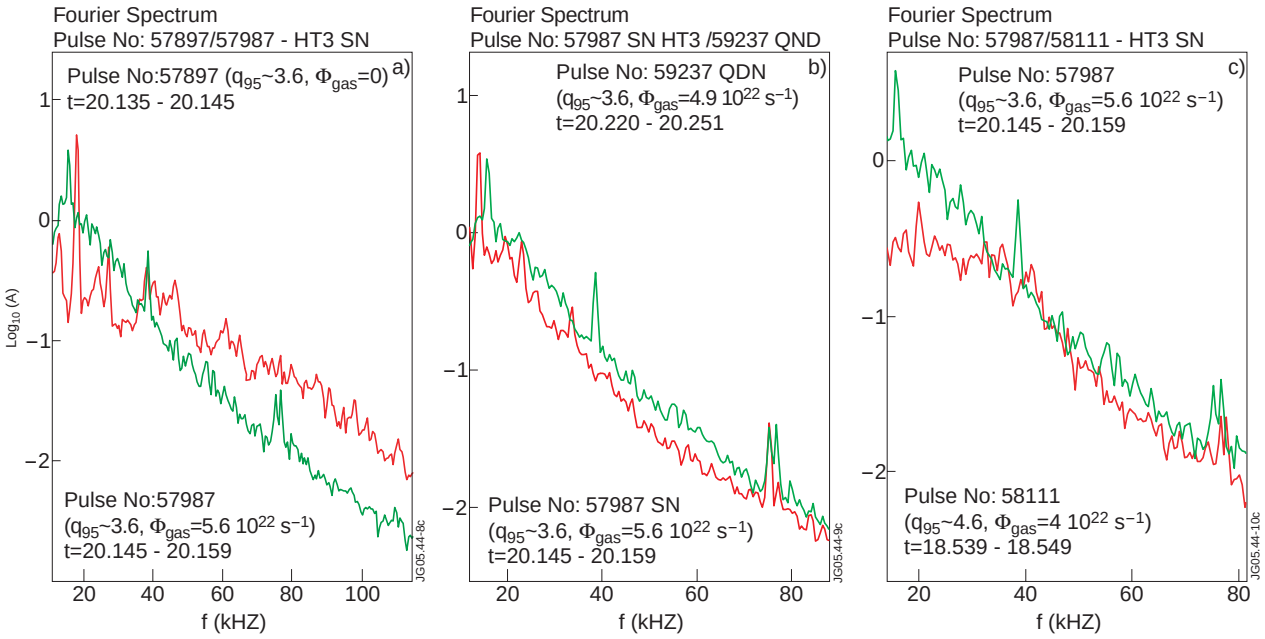

Figure 7: comparison of the intensity of MHD fluctuations and the W B modes for 3 pairs of pulses. Left, a): HT3 at low q Type I (red) and Type II (green); middle, b: SN HT3 vs. QDN1 at 2.5MA/2.7T, Type II phases; and last to the right, c), HT3 at low and high q_{95}. Note that the high frequency part of the spectrum is similar for both q_{95}, but the MHD fluctuations of the high q_{95} lacks the enhanced activity at low frequency, typical of Type II ELM phases.

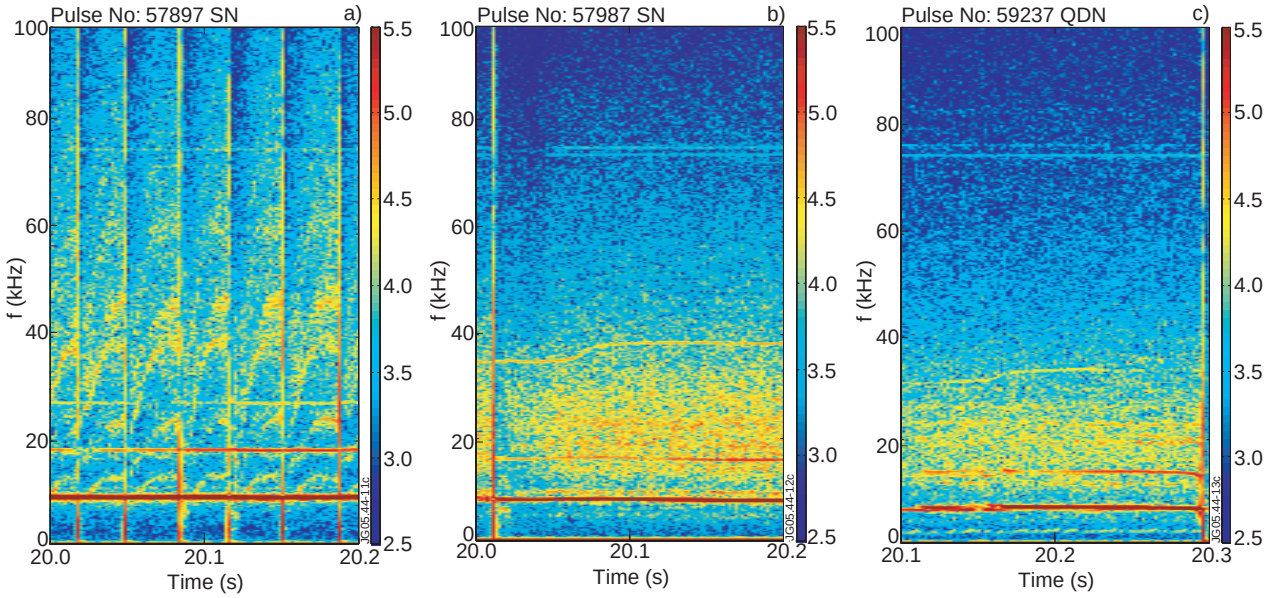

Figure 8: Spectrograms for 3 of the plasma pulses shown in Fig. 7. a) SN HT3 2.5MA/2.7T Type I (Pulse No: 57897); in the middle, b) HT3 2.5MA/2.7T with Type II ELMs (Pulse No: 57987), and last, c) QDN1 at 2.5MA/2.7T with Type II ELMs (Pulse No: 59237). The intense and narrow vertical bands are type I ELMs, the horizontal continuous narrow bands wiht high intensity are correlated to core MHD activity.

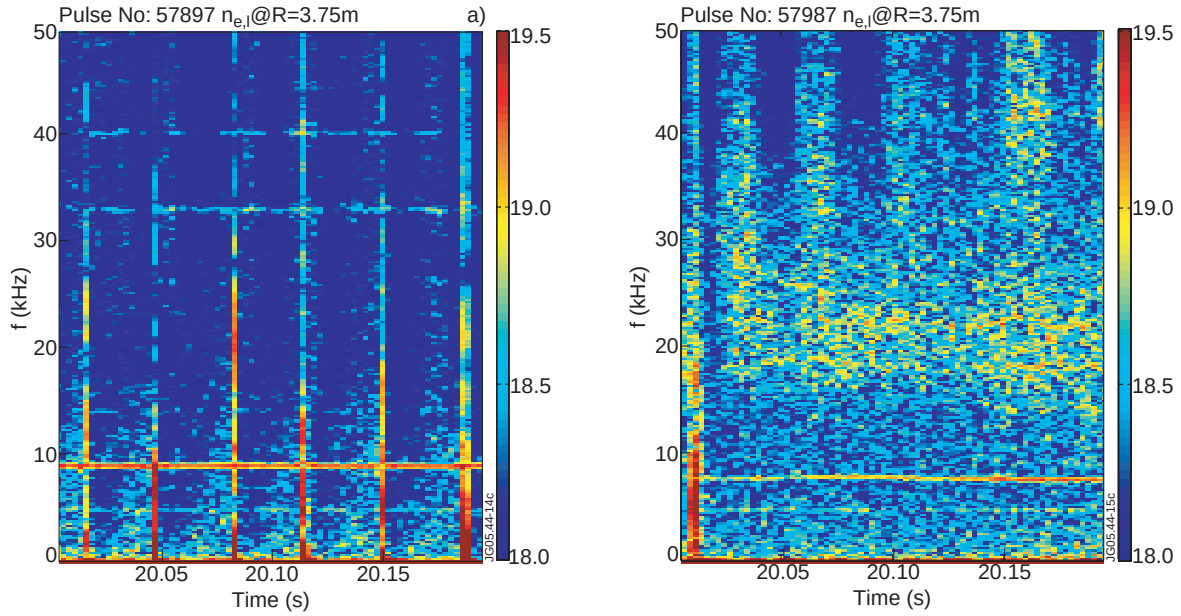

Figure 9: density fluctuation as measured by fast interferometry in SN, type I ELMy H-mode (a), and mixed Type I-II H-mode (b). Same discharges as for figure 8a and b.

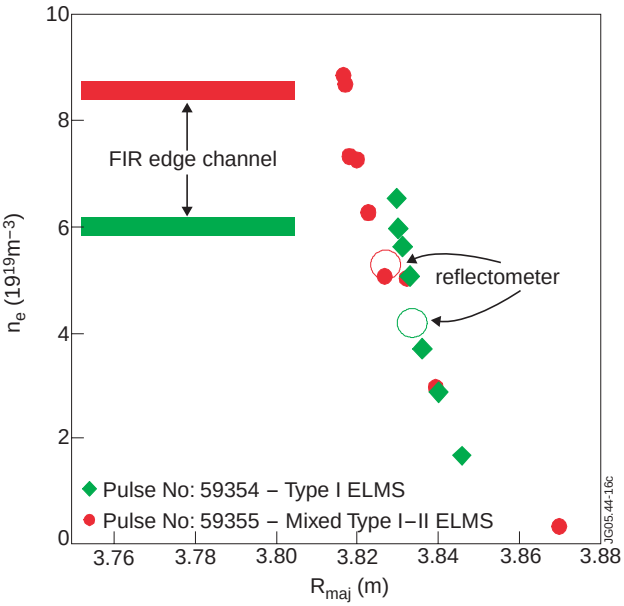

Figure 10: position of the cut-off density layer in the pedestal gradient region for 59354 (57897, HT3, Type I) and 59355 (57987, HT3, mixed Type I-II).

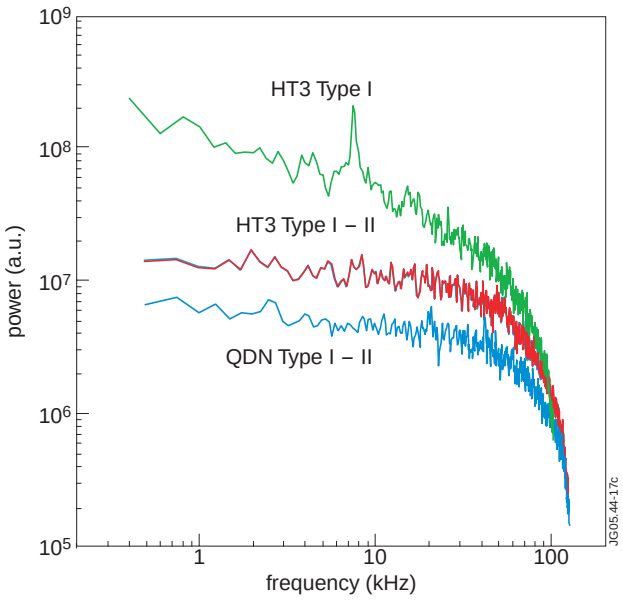

Figure 11: intensity of density fluctuations for pulses 57897 (green), 57987 (red), and for comparison, the QDN1 2.5MA/2.7T , 59237 (blue)

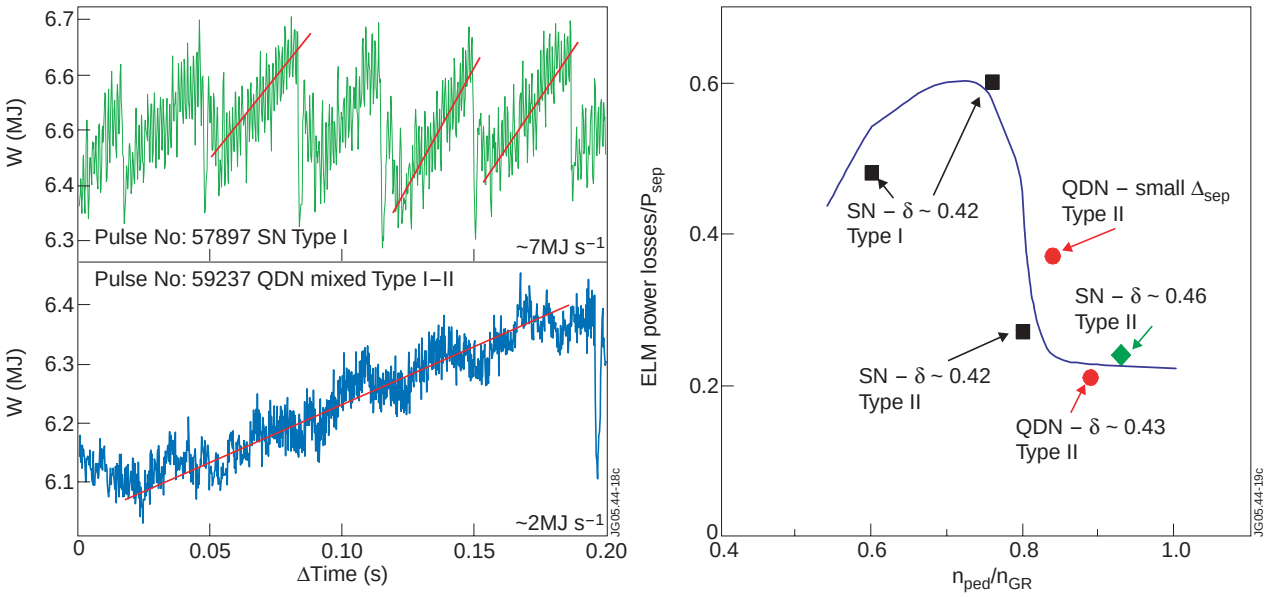

Figure 12: variation of the re-heating rate between ELMs with ELM type and configuration. Left side: comparison of the time evolution of the plasma stored energy for pulse 57897 (SN HT 3, 2.5MA/2.7T) with standard Type I ELMs, and that of pulse 59237 (QDN, 2.5MA/2.7T) with mixed Type I-II edge. Their magnetic fluctuation spectra are shown in Figs. 8a and b. Right side: fraction of the power across the separatrix carried by ELMs compared to the total loss power: this fraction decreases markedly in the mixed Type I-II regime, for both SN and QDN configurations.

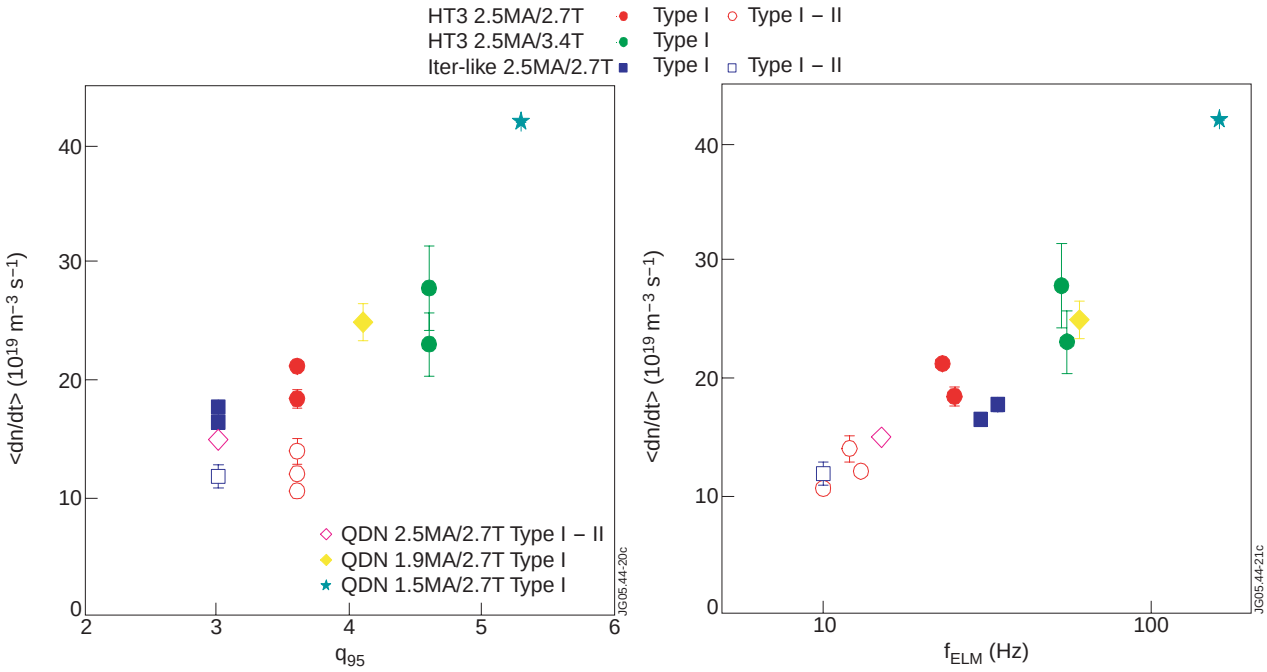

Figure 13: left: Comparison of the average net edge particle re-fuelling rate between Type I ELMs for SN HT 3, QDN, for various q_{95}. Right: Average net particle refuelling rate as function of the Type I ELM frequency, for the same set of data as the left plot in this figure.

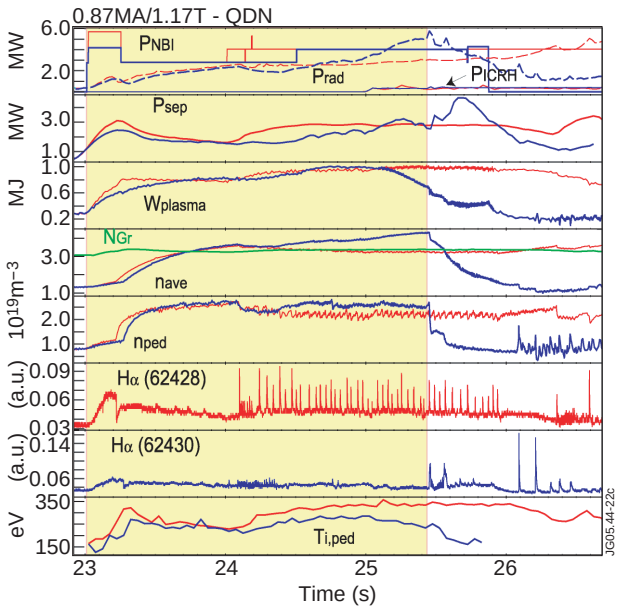

Figure 14: Selected time traces for 2 pulses of the JET / Asdex " U pgrade identity experiments: in red Pulse No: 62428 (Type I ELMs) and in blue, pulse 62430 (Type II ELMs). From top to bottom: NB and ICRH input powers (full lines, P_{NBI} and P_{ICRH}, MW) and total radiated power (dashed lines, P_{rad}, MW); power across the separatrix, P_{sep}, MW); plasma stored energy, W_{plasma} (MJ); line average density, n_{ave} and Greenwald density (green, n_{GR}); pedestal density n_{ped}, all in units of $10^{19}m^{-3}$; divertor H_a (Pulse No: 62428, a.u.); divertor H_α (Pulse No: 62430, a.u.) and, finally, pedestal temperature $T_{i,\,ped}$ (eV). The yellow box highlights the H-mode phase of Pulse No: 62430 until the loss of confinement due to core radiative collapse.

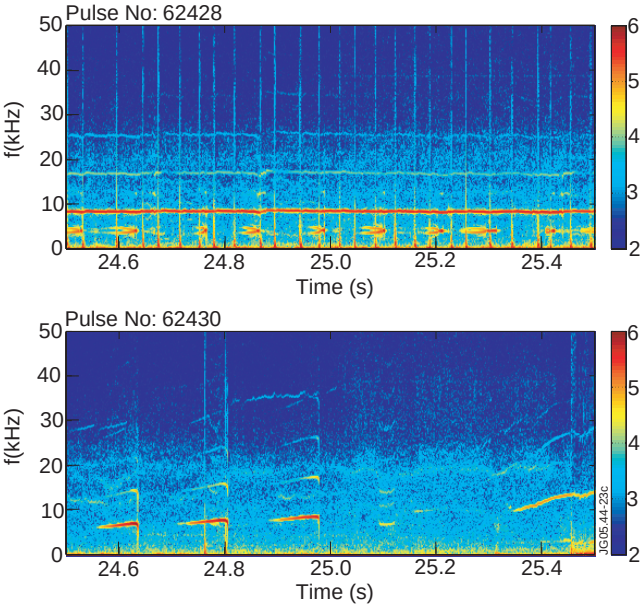

Figure 15: MHD spectrogrammes for the two plasma Pulse No: 62428 (top) and Pulse No: 62430 (bottom). The spectrogram for Pulse No: 62428 is typical of a Type I ELMy H-mode, while that of Pulse No: 62430, shows W B modes (continuous fluctuations in the 10 - 25kHz range) replacing the Type I ELM signature (the short, intense bursts of MHD are due to sawteeth).

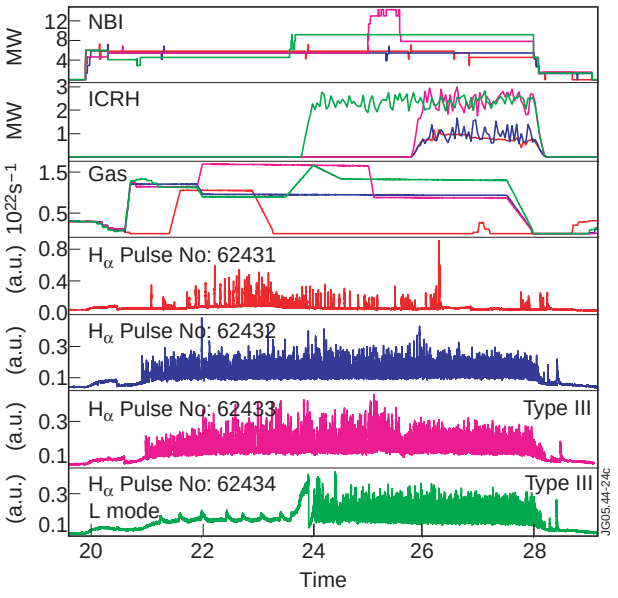

Figure 16: time traces for the power/gas scans carried out in the Asdex-Upgrade similarity experiments, for the 1.5MA/2T case, 4 pulses. Variation of injected power and fuelling were carried out in each pulse to explore the possible access to steady state Type II ELMy edge, not obtained. From top to bottom: NB injection power (MW), ICRH injected power (MW), gas injection ($10^{22}\ s^{-1}$), and divertor H_a traces for each of the pulses.

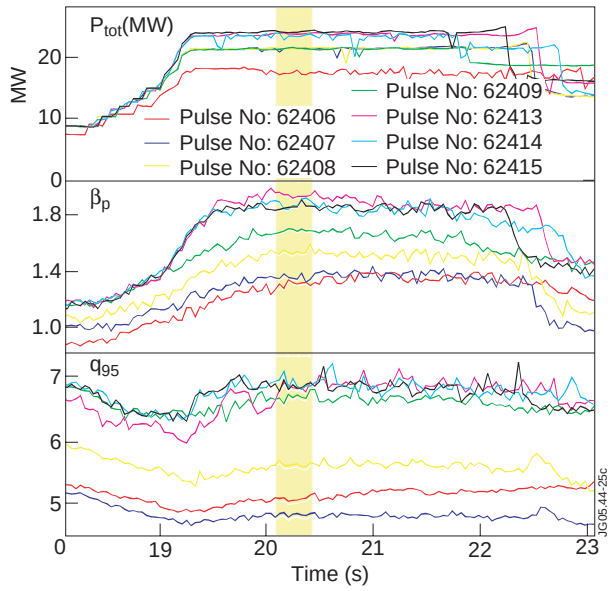

Figure 17: selected time traces for 7 plasma discharges of the high β_p H-mode scan. from top to bottom: total input power (NBI + ICRH, MW); β_p and q_{95}. The yellow stripe marks the time slice of the zoomed H_α traces in Fig. 18.

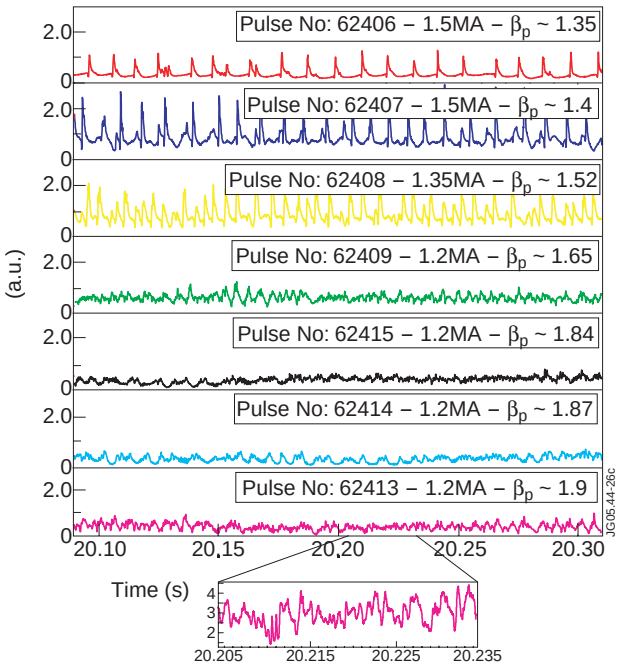

Figure 18: divertor H_α time traces for the β_p scan in high l_i H-modes (same plasma pulses and color code as Fig. 17). "Grassy" ELMs are observed for $\beta_p \gtrsim 1.6$ - 1.7. The 35ms zoom of the H_α trace of Pulse No: 62413 shows that the regular bursts typical of Type I ELM activity are absent.

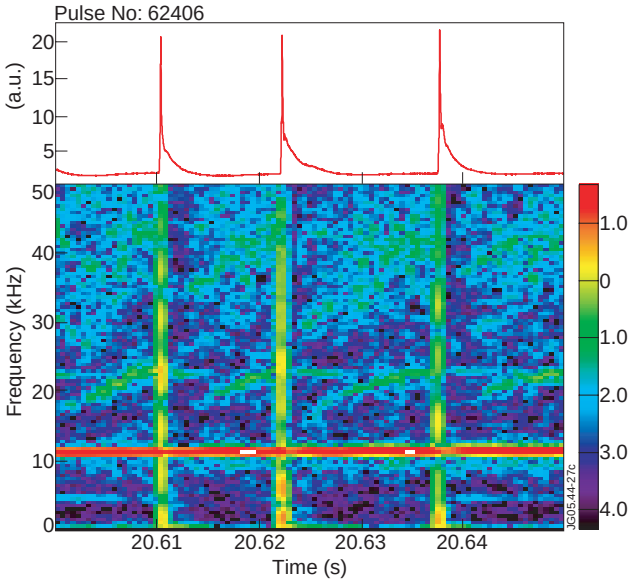

Figure 19: H_α time trace and MHD spectrogramme for Pulse No: 62406 (Type I ELMs, β_p ~ 1.35).

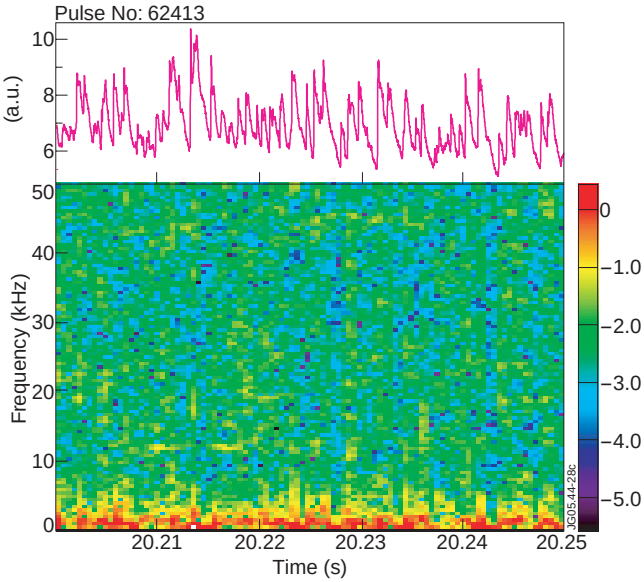

Figure 20: H_α time trace and MHD spectrogramme for Pulse No: 62413 ("grassy" ELMs, β_p ~ 1.9).

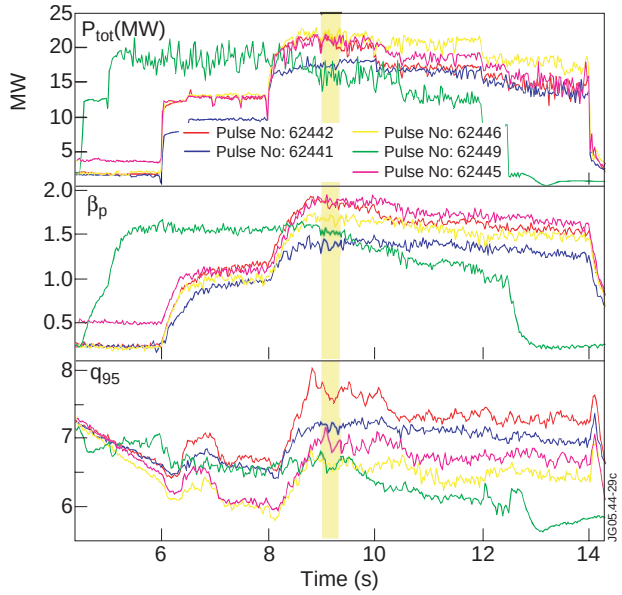

Figure 21: Selected time traces for 6 plasma pulses of the high β_p low l_i H-mode scan. From top to bottom: total input power (NBI + ICRH, MW); β_p and q_{95}. The yellow stripe marks the time slice of the zoomed H_α traces in figure.

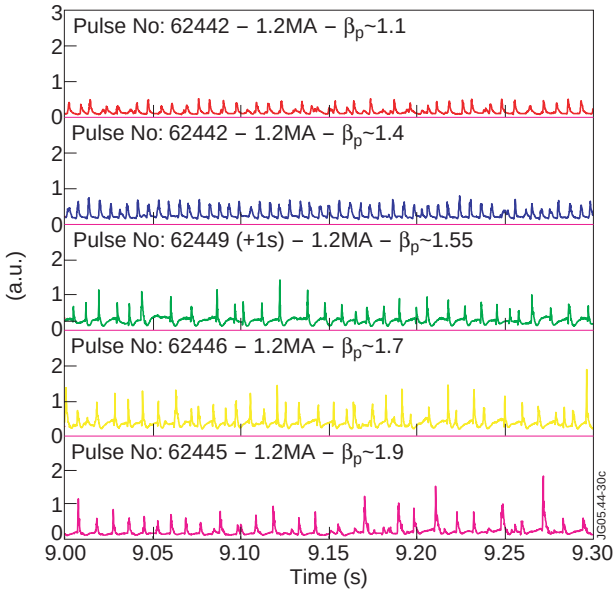

Figure 22: Divertor H_α time traces for the β_p scan in low l_i H-modes (same plasma discharges and color code as Fig. 21). Type I ELMs are observed for all β_p values.

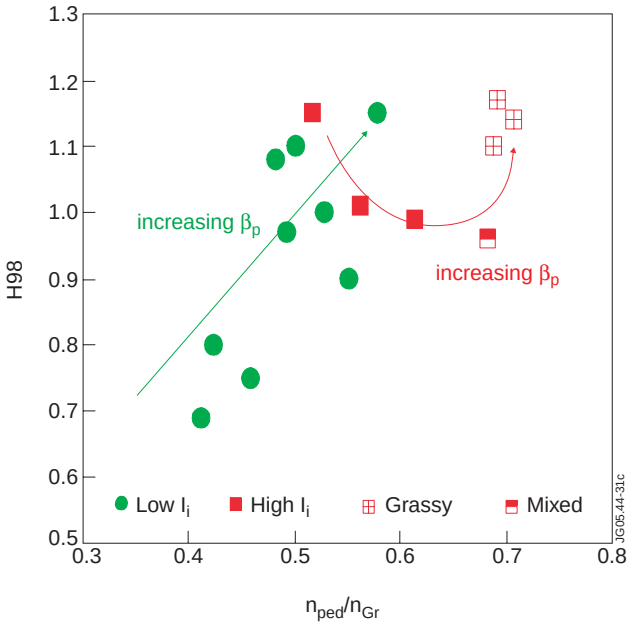

Figure 23: Confinement enhancement factor H_{98} as function of the normalised pedestal density n_{ped}/n_{GR}, for both high- and low l_i H-modes. Full symbols represents data points from H-modes with a Type I edge, half-full symbols are for H-modes with mixed periods of Type I and grassy ELMs, while the squares with crosses represent data point taken with a grassy ELMy edge. This symbol convention is maintained for all subsequent figures.

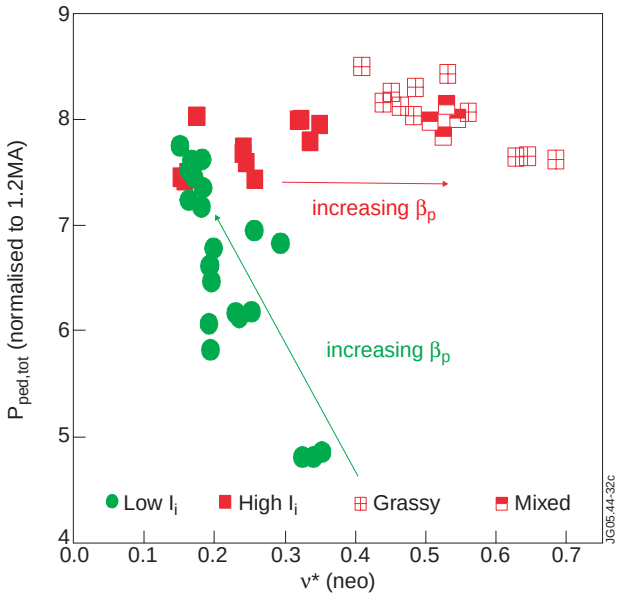

Figure 24: p_{ped} (normalised to I_p^2) for the high l_i and low l_i H-modes β_p scans.

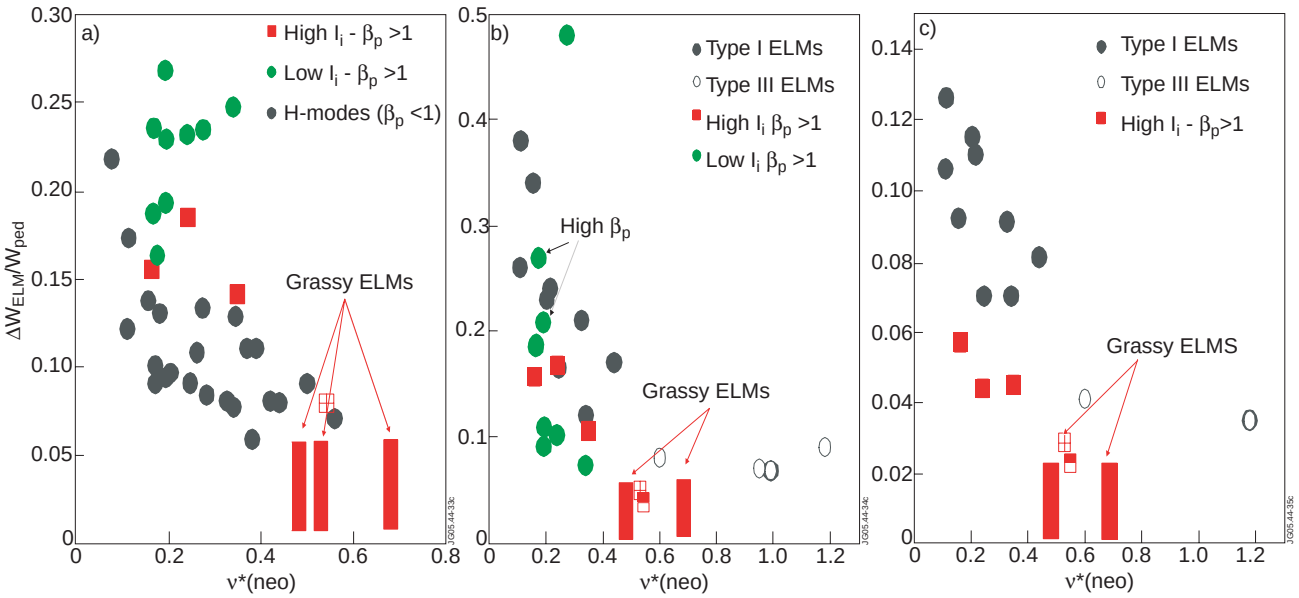

Figure 25: Summary of ELM losses for high β_p-high l_i, high β_p- low l_i and standard (β_p < 1) H-modes. a) ELM energy losses ΔW_{ELM} , normalised to the pedestal energy W_{ped}; b) pedestal electron temperature drop at the ELM, ΔT_{ELM}, normalised to $T_{e, ped}$; c) pedestal density drop at the ELM, $\Delta n_{e, ELM}$, normalised to the pedestal electron density ne. Standard H-modes in black (from [Loarte et al., 2004]), low li H-modes in green, high l_i H-modes in red. The red bars are calculated from estimated ΔW_{ELM}, ΔT_{ELM} and Δn_{ELM}, with the top of the bar being the upper value for those quantities.

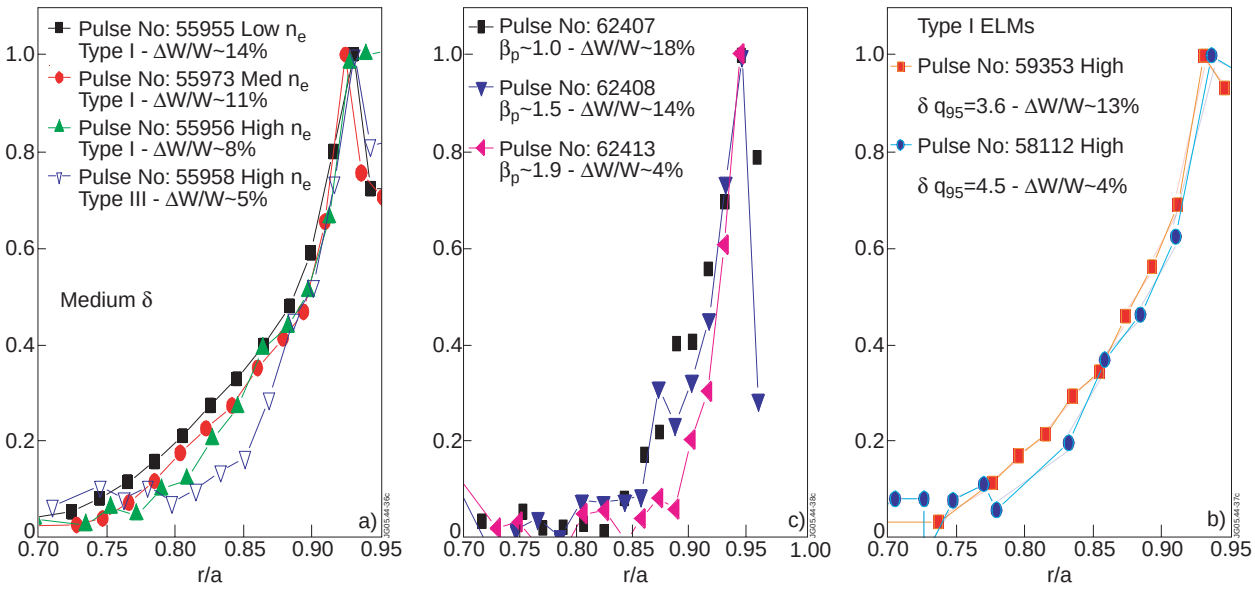

Figure 26: Perturbed T_e profiles for several H-mode discharges. a) density/gas scan in a medium δ ELMy H-mode at 2.5MA/2.4T, at constant P_{in}; full symbols Type I ELMs, open symbols, Type III ELMs. b) Comparison between the temperature profile perturbation of 2 HT3 pulsees at q_{95} = 3.6 and q_{95} = 4.5, both with Type I ELMs and, last to the right, c) for 3 pulses of the β_p scan, high l_i.

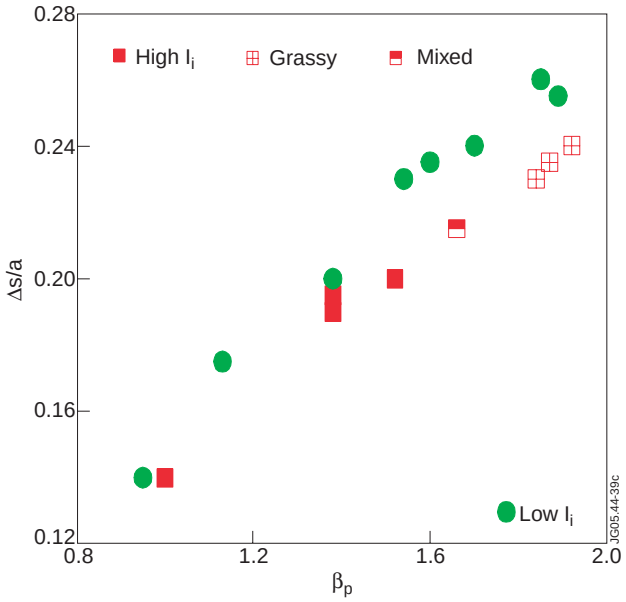

Figure 27: Shafranov shift (normalised to the plasma minor radius) Δ_S/a as function of β_p, for the β_p scan in the high l_i (squares) and in the low l_i H-modes (circles).

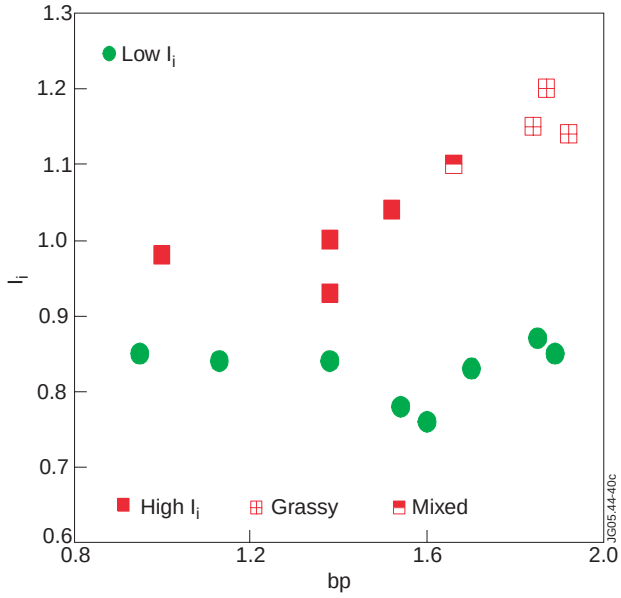

Figure 28: Internal inductance li as function of β_p, for the same set of pulses in Fig. 27.